Superexchange interaction between lanthanide f^1 ions. Spin-Hamiltonian calculations for the $90°$ and $180°$ $f^1 - f^1$ superexchange

1996 J. Phys.: Condens. Matter 8 10551

(http://iopscience.iop.org/0953-8984/8/49/042)

J. Phys.: Condens. Matter **8** (1996) 10551–10580. Printed in the UK

Superexchange interaction between lanthanide f^1 ions. Spin-Hamiltonian calculations for the 90° and 180° f^1–f^1 superexchange

V S Mironov

Institute of Crystallography, Russian Academy of Sciences, Leninskii prospekt 59, 117333 Moscow, Russia

Received 10 July 1995, in final form 4 September 1996

Abstract. Exchange interaction between two lanthanide or actinide ions of f^1 configuration bridged by common diamagnetic ligands is theoretically studied using a modified version of the superexchange theory developed in this paper. Exchange spin Hamiltonians were calculated for the M_2L_{10} and M_2L_{11} dimers serving as models of the 90° and 180° f^1–f^1 superexchange, respectively. Spin–orbit coupling and crystal field splitting of the f^1 configuration (resulting in the Γ_7 ground Kramers doublet and the effective spin $S = \frac{1}{2}$ of the metal ion), virtual transfers of electrons of the type 4f^1(A)–4f^1(B) $\rightarrow$ 4f^0(A)–4f^1(B)5d^1(B) via ns(L) and np(L) valent orbitals of the bridging ligands, and exchange pathways in these dimers are considered in detail. The f^1–f^1 superexchange is found to be extremely anisotropic and very sensitive to the geometry of the dimer. The spin Hamiltonian of the M_2L_{10} dimer is $H = J_x S_A^x S_B^x + J_y S_A^y S_B^y + J_z S_A^z S_B^z$, where the exchange parameters are rationalized in terms of $J_{\pi\sigma}$ and $J_{\pi\pi}$ parameters referring, respectively, to the π–σ and π–π pathways of the 4f(A) $\rightarrow$ np(L) $\rightarrow$ 5d(B) electron transfers, $J_x = 2J_{\pi\sigma} - J_{\pi\pi}$, $J_y = J_{\pi\sigma} + J_{\pi\pi}$ and $J_z = -J_{\pi\sigma} + J_{\pi\pi}$. The $J_{\pi\sigma}$ and $J_{\pi\pi}$ values are analytically expressed through $\langle 4\mathrm{f}|n\mathrm{p}\rangle$ and $\langle 5\mathrm{d}|n\mathrm{p}\rangle$ overlap integrals, orbital energies and intra-ionic Slater parameters. Exchange interaction between f^1 ions in the M_2L_{11} dimer is described by an antiferromagnetic Ising Hamiltonian $H = |J_{\pi\pi}| S_A^z S_B^z$, where the z axis connects two metal ions. Unusual magnetic properties of MUO_3 (M = Li, Na, K and Rb) and Li_3UO_4 oxides involving U^{5+}(5f^1) ions and $BaPrO_3$ distorted perovskite are discussed in the light of these theoretical results.

1. Introduction

Magnetic interactions between lanthanide or actinide ions (f ions) in non-metallic compounds are unusual and very complicated. It is generally recognized that strong magnetic anisotropy is an almost universal property of f-block-element compounds. Typical examples are rare-earth ortho-aluminates $LnAlO_3$ [1], garnets $Ln_3Al_5O_{12}$ [2], fluorides ($LiErF_4$) [3], chlorides $LnCl_3$ [4], hydroxides $Ln(OH)_3$ [5] and some actinide compounds such as MUO_3 and M_3UO_4 (M = Li or Na) [6, 7]. In some cases exchange interactions are so anisotropic that they cannot be rationalized even qualitatively in terms of the conventional isotropic Heisenberg Hamiltonian [8]. This is closely related to the unquenched orbital moment of f electrons and strong spin–orbit coupling. Detailed discussions of these problems have been given elsewhere [9].

Magnetic interactions between metal ions in insulators are usually described by superexchange via intermediate ligands [10, 11]. Although the general principles of the superexchange mechanism are essentially the same for f and d ions, calculations of exchange

0953-8984/96/4910551+30$19.50

parameters for lanthanides are more difficult than are those for transition metal compounds because of the complicated electronic structure of f^N ions in solids. As a consequence, little is still known about specific mechanisms of exchange interactions in actual lanthanide or actinide compounds despite exchange interactions between lanthanide ions in insulators having been studied for many years [12–18].

The aim of this paper is to analyse in detail the superexchange mechanism for pairs of f^1 ions, the simplest exchange systems. We calculate exchange spin Hamiltonians for M_2L_{10} and M_2L_{11} dimers (figure 1), in which f^1 ions M are bridged by two and one common ligands L, respectively. These dimers are convenient models to study the f^1–f^1 superexchange for the 90° and 180° geometries of the M–L–M bridges. By analogy with the Goodenough–Kanamori rules for the 90° and 180° superexchanges between d ions [19, 20], the comparative study of exchange spin Hamiltonians for these two dimers can be very informative for a deeper understanding of the nature of superexchange in lanthanides and, particularly, the origin of strong exchange anisotropy.

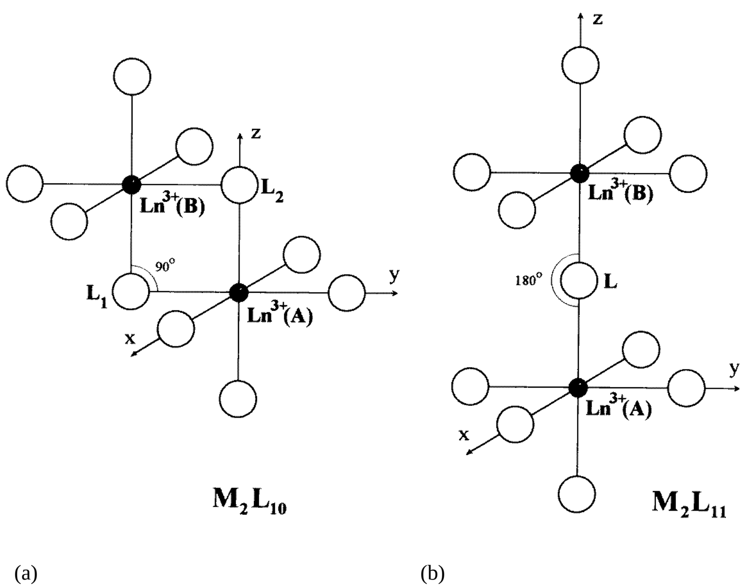

Figure 1. The structures of (a) M_2L_{10} and (b) M_2L_{11} dimers.

The paper is organized as follows. In section 2 a modified superexchange formalism for many-electron lanthanide ions of effective spin $S = \frac{1}{2}$ is developed. In section 3 this theory is used for calculations of spin Hamiltonians for the M_2L_{10} and M_2L_{11} f^1–f^1 dimers. We show that, for a correct description of the f^1–f^1 superexchange, a number of important factors should be taken into account, such as crystal field (CF) and spin–orbit splitting of the f^1 configuration, virtual transfers of electrons of the type $4f^1$–$4f^1 \rightarrow 4f^0$–$4f5d$ via bridging ligands, anisotropic overlap between metal and ligand orbitals, and specific electron transfer pathways. We show that both 90° and 180° f^1–f^1 superexchanges are very anisotropic despite the $\mathbf{g}$ tensor of the ground electronic level of each ion being isotropic. This demonstrates that strong exchange anisotropy in f systems is not necessarily due to the CF anisotropy. A discussion is given in section 4, in which some experimental data on magnetic properties of insulating compounds containing f^1 ions are considered in the light of the theoretical results of this paper.

2. The many-electron form of the superexchange theory for the effective spin $\mathbf{S} = \frac{1}{2}$

2.1. Preliminaries

It has become almost universal practice to use the second quantization technique in theoretical studies of exchange interactions between magnetic ions in insulators [10–16]. At this point we show that, for lanthanide and actinide ions, the traditional superexchange formalism based on the second quantization technique should be re-formulated in order to take into account specific features of the electronic structure of the f shell. To determine the requirements of this modified approach, we consider the main differences between the superexchange mechanisms for f ions and for d ions.

According to the superexchange theory [10, 11], coupling between magnetic moments of two metal ions A and B is due to virtual transfers of electrons of the type $AB \rightarrow A^+B^- \rightarrow AB$ via common bridging ligands, which result in mixing of wavefunctions of the ground homopolar state AB with wavefunctions of excited 'ionic' states A^+B^- and A^-B^+. For transition metal ions theoretical treatment of these charge-transfer processes is simpler, because the strong CF splitting of d orbitals leads to the fact that wavefunctions of transition metal ions are usually well described in the one-determinant approximation. In this case each wavefunction is defined by the set of occupied d orbitals, so the charge transfer process $AB \rightarrow A^+B^-$ can be simply regarded as transfer of an electron from $d_i(A)$ orbital of ion A to $d_j(B)$ orbital of ion B. These processes are effectively treated by the second quantization technique in terms of one-electron states.

The situation is, however, quite different for lanthanide and actinide ions. Except in a few special cases, the f^N shell is a strongly correlated electronic system, so its wavefunction cannot be described by one Slater determinant, even to first approximation. The ground state of a Ln^{3+} ion results from the CF splitting of the ground J manifold of the relevant f^N configuration and the corresponding wavefunction is a linear combination of a large number of determinants. In addition, for a pair of lanthanide ions $Ln(A)^{3+}$ and $Ln(B)^{3+}$ charge-transfer processes $AB \rightarrow A^+B^-$ involve not only the basic configurations $4f^{N_A}$ and $4f^{N_B}$ but also configurations with $N_A \pm 1$ and $N_B \pm 1$ electrons, such as $4f^{N_A-1}$, $4f^{N_B-1}$, $4f^{N_A}n'l'$ or $4f^{N_B}n'l'$ (where $n'l' = 4f$, 5d, 6s and so on). This leads to the fact that charge-transfer transition for lanthanide ions is no longer a simple electron transition between f orbitals $f_i(A) \rightarrow f_j(B)$, but should rather be regarded as a transition between two many-electron states of the joint electronic system of the exchange pair, $\Psi_i(4f^{N_A}, 4f^{N_B}) \rightarrow \Psi_j(4f^{N_A-1}, 4f^{N_B}n'l')$. Therefore, it is desirable to modify the superexchange theory for lanthanide ions in order to deal directly with many-electron eigenfunctions of the unperturbed pair rather than with f orbitals. Unfortunately, the second quantization technique is an ill-adapted one for this purpose because the second quantized Hamiltonian is written in terms of one- and two-electron matrix elements and electron creation and annihilation operators associated with a certain one-electron basis set. Description of $AB \rightarrow A^+B^- \rightarrow AB$ processes for a strongly correlated electronic system in terms of the second quantization technique leads to the necessity of considering numerous elementary exchange processes (like the $h : h$, $h_s : h_s$, $h : g$ and so on processes discussed in the review of Stevens [14]) associated with transfers of electrons between individual orbitals of magnetic ions and ligands. The main idea of our approach is to describe these exchange processes in a global way in terms of many-electron states of the unperturbed pair.

Like in any exchange theory, the first step is the determination of the unperturbed Hamiltonian and the perturbation for a pair of lanthanide ions. The unperturbed Hamiltonian should be chosen so that it describes the actual wavefunctions of separate lanthanide ions in the pair and is fully symmetrical with respect to interchanges of electrons. Usually only the ground and the lowest excited CF levels of a Ln^{3+} ion are involved in exchange interaction. In this work we develop a modified exchange formalism for the most important case, in which the ground CF state of an f ion is a Kramers doublet corresponding to the effective ionic spin $S = \frac{1}{2}$. It is important to note that CF splitting of J manifolds for lanthanide ions is of order 100 cm^{-1} and exchange parameters are normally of order within a few reciprocal centimetres [1–5]. This implies that exchange interaction has very little influence on wavefunctions of lanthanide ions which are formed under the combined action of intra-ionic interactions (attraction to nuclei, electron–electron repulsion and spin–orbit coupling) and the CF potential. It is therefore quite natural to use actual many-electron wavefunctions of lanthanide ions in a crystal as basis functions, that implies the involvement of the CF potential in the unperturbed Hamiltonian. These functions can be taken as antisymmetrized products of many-electron eigenfunctions of CF states of individual Ln^{3+} ions. It has been believed in some works [14] that the inclusion of the CF potential in the unperturbed Hamiltonian makes distinguishable electrons belonging to different magnetic ions, so the CF potential is incorporated into the perturbation. It should be pointed out, however, that our approach is free from this disadvantage because using antisymmetrized many-electron wavefunctions makes any Hamiltonian automatically symmetrical in electrons. Note also that the incorporation of such different terms as the CF potential ($\approx$ 100 cm^{-1}) and exchange interaction ($\approx$ 1 cm^{-1}) into a unique perturbation term can lead to some unwanted problems with convergence of the perturbation series. To ensure good convergence, the perturbation Hamiltonian should involve only those interactions which cause $AB \rightarrow A^+B^-$ or A^-B^+ electron transfer processes responsible for superexchange.

Another problem concerns the treatment of ligand electronic states. Some authors take into account the ligand's electrons together with electrons of magnetic ions in the perturbation procedure. This has the disadvantage that exchange terms appear in higher perturbation orders (fourth or even fifth) and, in addition, a part of the CF potential is incorporated into the perturbation [15, 16]. To avoid these difficulties, we follow the approach [10, 11] in which ligand states are excluded from consideration by the replacement of the actual unperturbed Hamiltonian by some effective unperturbed Hamiltonian acting only within the sub-space of f states. This allows one to confine consideration to the second-order perturbation.

Summarizing the aforesaid, we can formulate principles of the modified superexchange theory for lanthanides.

(i) The perturbation procedure for spin Hamiltonian calculations is formulated in terms of many-electron states of the unperturbed pair. For this reason we abandon the second quantization technique.

(ii) The spin Hamiltonian calculation procedure should lead directly to the exchange spin Hamiltonian.

(iii) The CF potential is incorporated into the unperturbed Hamiltonian of a lanthanide ion pair, while in the perturbation are involved only those interactions which are responsible for electron transfers between magnetic ions.

(iv) The ligand's electrons are not involved in the perturbation procedure.

In fact, this approach follows the principles of Anderson's superexchange theory [10, 11], according to which wavefunctions of CF levels of magnetic ions are determined beforehand by spin Hamiltonian calculations and ligand states are excluded. It differs from the traditional superexchange theory in that many-electron wavefunctions of magnetic ions are used rather than their one-electron states. Our modification is intended to adapt the superexchange formalism to magnetic ions with strongly correlated electronic states, such as lanthanide ions in crystals. Although ligand states are not involved directly in the perturbation calculations, special care is taken to relate transfer integrals to the geometry of Ln^{3+}(A)–L–Ln^{3+}(B) exchange bridges and to the electronic structure of the bridging ligands.

2.2. The many-electron superexchange formalism

We consider an exchange pair, which involves two metal ions A and B bridged by common diamagnetic ligands (namely non-metal ions having a closed $n\mathrm{s}^2n\mathrm{p}^6$ electronic shell) and some non-bridging ligands around each metal ion. To make the consideration more specific (but without loss of generality), hereafter we imply only lanthanide ions. The following general conditions are assumed.

(i) Ions A and B have odd numbers of f electrons (N_A and N_B, respectively). The ground CF state of each ion is a Kramers doublet that corresponds to the effective ionic spin $S = \frac{1}{2}$.

(ii) Only the ground CF state of each ion is involved in exchange interaction. This implies that the energy gap between the ground and first excited CF levels is much larger than the exchange parameters, so interionic exchange interactions do not mix the wavefunctions of the ground and excited CF states.

2.2.1. The unperturbed Hamiltonian and the perturbation. Consider the full electronic Hamiltonian of the exchange cluster (two metal ions A and B plus ligands) acting in the Hilbert space, whose basis set consists of Slater determinants involving all possible combinations of magnetically active spin orbitals of lanthanide ions A and B (4f, 5d and so on), as well as ns and np valent orbitals of ligands. All atomic orbitals in the determinants are assumed to be orthonormal. We use the well-known NDO (neglect of differential overlap) approximation, according to which two orbitals belonging to different atoms are orthogonal. This approximation is quite relevant to lanthanides because 4f orbitals overlap poorly with the environment.

Define the sub-space X, the basis set of which incorporates all determinants satisfying the following conditions.

(i) All valent spin orbitals of ligands are completely occupied by electrons; that is, each ligand has a closed $n\mathrm{s}^2n\mathrm{p}^6$ shell.

(ii) The sum $n(\mathrm{A}) + n(\mathrm{B}) = N_A + N_B$ is fixed, where $n(\mathrm{A})$ and $n(\mathrm{B})$ are the numbers of electrons on metal ions A and B. The number $n(\mathrm{A})$ can take the values $N_A - 1$, N_A and $N_A + 1$, and $n(\mathrm{B})$ can be $N_B - 1$, N_B or $N_B + 1$.

(iii) To each $n(\mathrm{A})$ there corresponds a certain electronic configuration on ion A:

$$n(\mathrm{A}) = N_A - 1 \qquad 4\mathrm{f}^{N_A-1}$$
$$n(\mathrm{A}) = N_A \qquad 4\mathrm{f}^{N_A}$$
$$n(\mathrm{A}) = N_A + 1 \qquad 4\mathrm{f}^{N_A}n'l'$$

where $n'l' =$ 4f, 5d, 6s and so on). The same is true for ion B.

The effective Hamiltonian $\mathbf{H}_1$ of the exchange pair is obtained by projection of the original Hamiltonian $\mathbf{H}$ acting in the full Hilbert space onto the sub-space X defined above. Formally, this projection corresponds to elimination of electronic variables of the ligand from consideration, because in the space X the electronic sub-system of ligands is described by only one configuration with a closed ns^2np^6 shell on each ligand. This, however, does not distinguish between ligands' and metals' electrons because of the antisymmetry of the wavefunctions of the basis set. Within the space X the Hamiltonian $\mathbf{H}_1$ is equivalent to the original Hamiltonian $\mathbf{H}$ (in particular, their energy spectra are identical).

To define the effective unperturbed Hamiltonian and the perturbation, the space X is divided into two sub-spaces X_1 and X_2 (so that $X = X_1 + X_2$), the first of which corresponds to wavefunctions of the basic homopolar state AB with $n(\mathrm{A}) = N_A$ and $n(\mathrm{B}) = N_B$ (the $4f^{N_A}$–$4f^{N_B}$ configuration). Subspace X_2 corresponds to ionic states A^+B^- and A^-B^+ ($4f^{N_A-1}$– $4f^{N_B}n'l'$ or $4f^{N_A}n'l'$–$4f^{N_B-1}$ configurations). We transform $\mathbf{H}_1$ to the Hamiltonian $\mathbf{H}_2$ by $\mathbf{H}_2 = \mathbf{T}\mathbf{H}_1\mathbf{T}^{-1}$, where $\mathbf{T}$ is a transformation diagonalizing $\mathbf{H}_1$ within each of the blocks X_1 and X_2. The diagonal part ($\mathbf{H}_0$) of $\mathbf{H}_2$ is regarded as the unperturbed Hamiltonian, the off-diagonal part $\mathbf{H}_{AB}$ as the perturbation,

$$\mathbf{H}_2 = \mathbf{H}_0 + \mathbf{H}_{AB}. \tag{1}$$

Being defined in such a way, the unperturbed Hamiltonian $\mathbf{H}_0$ involves all intra-ionic interactions on each ion A and B (interaction with the core potential of lanthanide ions, electron–electron repulsion and spin–orbit energy), as well as all metal–ligand interactions responsible for CF splitting on each ion. In addition, $\mathbf{H}_0$ incorporates that part of the interaction between ions (g_{AB}) which leaves unaltered the numbers $n(\mathrm{A})$ and $n(\mathrm{B})$ in ions A and B. For basic homopolar states AB this interaction is reduced to electric multipole–multipole interactions between 4f electrons on different ions, as well as to the direct exchange interaction J_{AB}, whose value is given by

$$J_{AB} \approx \int \frac{\phi_i^A(\boldsymbol{r}_1)^*\phi_j^B(\boldsymbol{r}_2)^*\phi_i^A(\boldsymbol{r}_2)\phi_j^B(\boldsymbol{r}_1)}{|\boldsymbol{r}_1 - \boldsymbol{r}_2|}\,\mathrm{d}\boldsymbol{r}_1\,\mathrm{d}\boldsymbol{r}_2 \tag{2}$$

where $\phi_i^A(\boldsymbol{r}_1)$, $\phi_j^B(\boldsymbol{r}_2)$, $\phi_i^A(\boldsymbol{r}_2)$ and $\phi_j^B(\boldsymbol{r}_1)$ are 4f orbitals of ions A and B. For a typical distance of 4 Å between two nearest lanthanide ions in an insulating crystal, J_{AB} is negligibly small because the product $\phi_i^A(\boldsymbol{r})^*\phi_j^B(\boldsymbol{r})$ is almost zero elsewhere. The situation is, however, different for A^+B^- and A^-B^+ states (sub-space X_2). In this case g_{AB} involves interaction between the hole on ion A (the $4f^{N_A-1}$ configuration) and the extra electron on ion B (the $4f^{N_B}n'l'$ configuration). Although this interaction is larger ($g_{AB} \approx 1$–2 eV) than multipole–multipole or direct exchange interactions, it is however, significantly smaller than the energy separation between AB and A^+B^- states (≈ 10 eV).

In fact, the Hamiltonian $\mathbf{H}_0$ describes the electronic states of two weakly coupled lanthanide ions A and B, whose wavefunctions are very slightly affected by the neighbouring metal ion. This means that the eigenfunctions of $\mathbf{H}_0$ are well approximated by products of many-electron wavefunctions χ^A and χ^B of individual ions A and B

$$\begin{aligned}
&\Psi_{nm}(4f^{N_A}, 4f^{N_B}) = \chi_m^A(4f^{N_A})\chi_n^B(4f^{N_B})\\
&\Psi_{mn}(4f^{N_A-1}, 4f^{N_B}n'l') = \chi_m^A(4f^{N_A-1})\chi_n^B(4f^{N_B}n'l')\\
&\Psi_{mn}(4f^{N_A}n'l', 4f^{N_B-1}) = \chi_m^A(4f^{N_A}n'l')\chi_n^B(4f^{N_B-1})
\end{aligned} \tag{3}$$

where the double index mn reflects the genealogy of the corresponding two-ion wavefunction. To make all electrons indistinguishable, the wavefunctions are antisymmetrized over all electronic variables, $\chi_m^A\chi_n^B \rightarrow [\chi_m^A\chi_n^B]_{as}$. Below we omit the symbol of antisymmetrization $[\ldots]_{as}$, implying that products of two single-ion wavefunctions are always antisymmetrized.

The perturbation $\mathbf{H}_{AB}$ incorporates all interactions which cause electron transfers $AB \rightarrow A^+B^-$ or A^-B^+. Its matrix elements $\langle\Psi_{kl}(4f^{N_A}, 4f^{N_B})|\mathbf{H}_{AB}|\Psi_{mn}(4f^{N_A-1}, 4f^{N_B}n'l')\rangle$

connect homopolar states AB with ionic states A^+B^- or A^-B^+ (by definition, all non-vanishing matrix elements of this type are in the crossing of blocks X_1 and X_2 in the space $X = X_1 + X_2$). It is important to note that H_{AB} is mainly a one-electron operator h_{AB}:

$$\mathsf{H}_{AB} = \sum_{i=1}^{N_A+N_B} \mathsf{h}_{AB}(i) \tag{4}$$

because matrix elements of its two-electron part are proportional to overlap integrals of the type $\langle 4f(A)|n'l'(B)\rangle$, which are negligibly small for two neighbouring lanthanide ions. Therefore, matrix elements $\langle \Psi_{kl}(4f^{N_A}, 4f^{N_B})|\mathsf{H}_{AB}|\Psi_{mn}(4f^{N_A-1}, 4f^{N_B}n'l')\rangle$ can be expressed in terms of one-electron matrix elements $\langle 4f_i(A)|\mathsf{h}_{AB}|n'l'_j(B)\rangle = t_{ij}(4f, n'l')$ connecting 4f orbitals of ion A and $n'l'$ orbitals of ion B. Quantities t_{ij} are usually called transfer integrals and their origin is discussed in section 2.4. Expand the single-ion wavefunctions χ_m^A and χ_n^B into the series of Slater determinants

$$\begin{aligned}
\chi_k^A(4f^{N_A}) &= \sum_{p_A} C_k^A(\boldsymbol{p}_A)\,\mathrm{Det}(\boldsymbol{p}_A)\\
\chi_l^B(4f^{N_B}) &= \sum_{p_B} C_l^B(\boldsymbol{p}_B)\,\mathrm{Det}(\boldsymbol{p}_B)\\
\chi_m^A(4f^{N_A-1}) &= \sum_{q_A} C_m^A(\boldsymbol{q}_A)\,\mathrm{Det}(\boldsymbol{q}_A)\\
\chi_n^B(4f^{N_B}n'l') &= \sum_{u_B} C_n^B(\boldsymbol{u}_B)\,\mathrm{Det}(\boldsymbol{u}_B)
\end{aligned} \tag{5}$$

where the sums run over vector indexes $\boldsymbol{p}_A$, $\boldsymbol{p}_B$, $\boldsymbol{q}_A$ and $\boldsymbol{u}_B$, which are sets of quantum numbers of 4f and $n'l'$ orbitals involved in the corresponding Slater determinants $\mathrm{Det}(\boldsymbol{p}_A)$, $\mathrm{Det}(\boldsymbol{p}_B)$, $\mathrm{Det}(\boldsymbol{q}_A)$ and $\mathrm{Det}(\boldsymbol{u}_B)$:

$$\begin{aligned}
\boldsymbol{p}_A &= (4f_{k_1}(A), \ldots 4f_{k_{N_A}}(A))\\
\boldsymbol{p}_B &= (4f_{k_1}(B), \ldots 4f_{k_{N_B}}(B))\\
\boldsymbol{q}_A &= (4f_{k_1}(A), \ldots 4f_{k_{N_A-1}}(A))\\
\boldsymbol{u}_B &= (4f_{k_1}(B), \ldots 4f_{k_{N_B}}(B), n'l'_{k_{N_B+1}}(B)).
\end{aligned} \tag{6}$$

Quantities $C_k^A(\boldsymbol{p}_A)$, $C_l^B(\boldsymbol{p}_B)$, $C_m^A(\boldsymbol{q}_A)$ and $C_n^B(\boldsymbol{u}_B)$ in (5) are the expansion coefficients. Similarly, for two-ion wavefunctions we have

$$\begin{aligned}
\Psi_{kl}(4f^{N_A}, 4f^{N_B}) &= \sum_{p_A}\sum_{p_B} C_k^A(\boldsymbol{p}_A)C_l^B(\boldsymbol{p}_B)\,\mathrm{Det}(\boldsymbol{p}_A + \boldsymbol{p}_B)\\
\Psi_{mn}(4f^{N_A-1}, 4f^{N_B}n'l') &= \sum_{q_A}\sum_{u_B} C_m^A(\boldsymbol{q}_A)C_n^B(\boldsymbol{u}_B)\,\mathrm{Det}(\boldsymbol{q}_A + \boldsymbol{u}_B)
\end{aligned} \tag{7}$$

where $\boldsymbol{p}_A + \boldsymbol{p}_B$ and $\boldsymbol{q}_A + \boldsymbol{u}_B$ are vector indices of Slater determinants for the joint electronic system A + B:

$$\begin{aligned}
\boldsymbol{p}_A + \boldsymbol{p}_B &= (4f_{k1}(A), \ldots 4f_{k_{N_A}}(A), 4f_{k_{N_A+1}}(B), \ldots 4f_{k_{N_A+N_B}}(B))\\
\boldsymbol{q}_A + \boldsymbol{u}_B &= (4f_{k1}(A), \ldots 4f_{k_{N_A-1}}(A), 4f_{k_{N_A}}(B), \ldots 4f_{k_{N_A+N_B-1}}(B), n'l'_{k_{N_A+N_B}}(B)).
\end{aligned} \tag{8}$$

We can therefore write

$$\begin{aligned}
\langle \Psi_{k1}(4f^{N_A}, 4f^{N_B})|\mathsf{H}_{AB}|\Psi_{mn}(4f^{N_A-1}, 4f^{N_B}n'l')\rangle &= \sum_{p_A}\sum_{p_B}\sum_{q_A}\sum_{u_B} C_k^A(\boldsymbol{p}_A)^* C_1^B(\boldsymbol{p}_B)^* C_m^A(\boldsymbol{q}_A)\\
&\quad\times C_n^B(\boldsymbol{u}_A)\langle\,\mathrm{Det}(\boldsymbol{p}_A + \boldsymbol{p}_B)|\mathsf{H}_{AB}|\,\mathrm{Det}(\boldsymbol{q}_A + \boldsymbol{u}_B)\rangle.
\end{aligned} \tag{9}$$

This sum is easy to calculate because the matrix elements $\langle\,\mathrm{Det}(\boldsymbol{p}_A+\boldsymbol{p}_B)|\mathbf{H}_{AB}|\,\mathrm{Det}(\boldsymbol{q}_A+\boldsymbol{u}_B)\rangle$ are non-zero only if the determinants $\mathrm{Det}(\boldsymbol{p}_A+\boldsymbol{p}_B)$ and $\mathrm{Det}(\boldsymbol{q}_A+\boldsymbol{u}_B)$ differ from each other by no more than two orbitals $4\mathrm{f}_i(\mathrm{A})$ and $n'l'_j(\mathrm{B})$

$$\langle\,\mathrm{Det}(\boldsymbol{p}_A+\boldsymbol{p}_B|\mathbf{H}_{AB}|\,\mathrm{Det}(\boldsymbol{q}_A+\boldsymbol{u}_B)\rangle = \langle 4\mathrm{f}_i(\mathrm{A})|\mathbf{h}_{AB}|n'l'_j(\mathrm{B})\rangle = t_{ij}(4\mathrm{f}, n'l'). \tag{10}$$

Note that the one-electron operator $\mathbf{H}_{eff}$ is equivalent to the well-known second quantized 'kinetic' operator widely used in theoretical studies of exchange interactions in insulators [10–16].

2.2.2. The spin Hamiltonian calculation procedure. Denote $\varphi_A^{\pm} = \chi_0^A(4\mathrm{f}^{N_A})^{\pm}$ and $\varphi_B^{\pm} = \chi_0^B(4\mathrm{f}^{N_B})^{\pm}$ for wavefunctions of the ground CF level of ions A and B (where superscripts '+' and '−' stand for two components of the ground Kramers doublets). Our aim is to obtain an effective exchange Hamiltonian $\mathbf{H}_{eff}$ from the Hamiltonian $\mathbf{H}_2 = \mathbf{H}_0+\mathbf{H}_{AB}$, which describes the energy spectrum of the pair of lanthanide ions in the vicinity of its ground state. $\mathbf{H}_{eff}$ acts within the space of wavefunctions of the fourfold degenerate ground level of the unperturbed Hamiltonian $\mathbf{H}_0$

$$\varphi_A^+\varphi_B^+ \qquad \varphi_A^-\varphi_B^- \qquad \varphi_A^+\varphi_B^- \qquad \varphi_A^-\varphi_B^+. \tag{11}$$

Because of the time-reversal symmetry, the Hamiltonian $\mathbf{H}_{eff}$ is to be invariant with respect to the corresponding transformations of spin $S=\frac{1}{2}$ components, $(\varphi_A^+)^* \to \varphi_A^-$, $(\varphi_A^-)^* \to -\varphi_A^+$, $(\varphi_B^+)^* \to \varphi_B^-$ and $(\varphi_B^-)^* \to -\varphi_B^+$. Therefore, within the basis set (11) $\mathbf{H}_{eff}$ is represented by the following 4×4 matrix:

$$\mathbf{H}_{eff}\begin{pmatrix}\varphi_A^+\varphi_B^+\\ \varphi_A^-\varphi_B^-\\ \varphi_A^+\varphi_B^-\\ \varphi_A^-\varphi_B^+\end{pmatrix} = \begin{pmatrix} X & a & c & d\\ a^* & X & -d^* & -c^*\\ c^* & -d & Y & b\\ d^* & -c & b^* & Y\end{pmatrix}\begin{pmatrix}\varphi_A^+\varphi_B^+\\ \varphi_A^-\varphi_B^-\\ \varphi_A^+\varphi_B^-\\ \varphi_A^-\varphi_B^+\end{pmatrix}. \tag{12}$$

This Hamiltonian can be obtained from the full effective Hamiltonian $\mathbf{H}_0+\mathbf{H}_{AB}$ (acting in the space $\mathrm{X}=\mathrm{X}_1+\mathrm{X}_2$) by its projection onto the sub-space (11). Because $\mathbf{H}_{AB}$ has no diagonal matrix elements, first-order perturbation does not contribute to $\mathbf{H}_{eff}$. In the second-order perturbation $\mathbf{H}_{eff}$ is obtained with the well-known formula for degenerate levels

$$\mathbf{H}_{eff} = \sum_{i\neq 0}\frac{\mathbf{P}_0\mathbf{H}_{AB}\mathbf{P}_i\mathbf{H}_{AB}\mathbf{P}_0}{E_0-E_i} \tag{13}$$

where

$$\mathbf{P}_0 = \sum_{n_0}|n_0\rangle\langle n_0| \qquad \mathbf{P}_i = \sum_{n_i}|n_i\rangle\langle n_i|$$

are projection operators for the ground level E_0 and excited levels E_i, respectively. The latter are charge-transfer states $\mathrm{A^+B^-}$ and $\mathrm{A^-B^+}$, whose wavefunctions we denote for brevity $Q_{mn}(\mathrm{A}\to\mathrm{B}) = \Psi_{mn}(4\mathrm{f}^{N_A-1}, 4\mathrm{f}^{N_B}n'l')$ and $Q_{mn}(\mathrm{B}\to\mathrm{A}) = \Psi_{mn}(4\mathrm{f}^{N_A}n'l', 4\mathrm{f}^{N_B-1})$. The matrix elements of the 4×4 matrix (12) of the exchange Hamiltonian $\mathbf{H}_{eff}$ are defined by the equation

$$\begin{aligned}\langle pq|\mathbf{H}_{eff}|rs\rangle = &-\sum_{Q_{mn}(A\to B)}\frac{\langle pq|\mathbf{H}_{AB}|Q_{mn}(\mathrm{A}\to\mathrm{B})\rangle\langle Q_{mn}(\mathrm{A}\to\mathrm{B})|\mathbf{H}_{AB}|rs\rangle}{E_{mn}(\mathrm{A}\to\mathrm{B})}\\ &-\sum_{Q_{mn}(B\to A)}\frac{\langle pq|\mathbf{H}_{AB}|Q_{mn}(\mathrm{B}\to\mathrm{A})\rangle\langle Q_{mn}(\mathrm{B}\to\mathrm{A})|\mathbf{H}_{AB}|rs\rangle}{E_{mn}(\mathrm{B}\to\mathrm{A})}\end{aligned} \tag{14}$$

where $p, r = \varphi_A^{\pm}$ and $q, s = \varphi_B^{\pm}$. The sums range over all charge-transfer states $Q_{mn}(\mathrm{A} \to \mathrm{B})$ and $Q_{mn}(\mathrm{B} \to \mathrm{A})$. Quantities $E_{mn}(\mathrm{A} \to \mathrm{B})$ and $E_{mn}(\mathrm{B} \to \mathrm{A})$ in the denominators are charge-transfer energies, which are the differences between eigenvalues of the unperturbed Hamiltonian $\mathbf{H}_0$ for the ground state $\varphi_A^{\pm}\varphi_B^{\pm} = \chi_0^A(4\mathrm{f}^{N_A})^{\pm}\chi_0^B(4\mathrm{f}^{N_B})^{\pm}$ and excited ionic states $Q_{mn}(\mathrm{A} \to \mathrm{B}) = \chi_m^A(4\mathrm{f}^{N_A-1})\chi_n^B(4\mathrm{f}^{N_B}n'l')$ or $Q_{mn}(\mathrm{B} \to \mathrm{A}) = \chi_m^A(4\mathrm{f}^{N_A}n'l')\chi_n^B(4\mathrm{f}^{N_B-1})$. Matrix elements $\langle\varphi_A^{\pm}\varphi_B^{\pm}|\mathbf{H}_{AB}|Q_{mn}(\mathrm{A} \to \mathrm{B})\rangle$ in the nominators of (14) are calculated with equations (7) and (9). It is important to note that this perturbation series has a good convergence, because in lanthanide systems transfer integrals $t_{ij}(4\mathrm{f}, n'l')$ are typically of 0.1 eV (see section 3.5), whereas charge-transfer energies are about 10 eV.

$\mathbf{H}_{eff}$ can be transformed to the conventional exchange spin Hamiltonian written in terms of components of the effective spin $S = \frac{1}{2}$ of ions A and B, which are defined by

$$S_n^x\varphi_n^{\pm} = \tfrac{1}{2}\varphi_n^{\mp} \qquad S_n^y\varphi_n^{\pm} = \mp(\mathrm{i}/2)\varphi_n^{\mp} \qquad S_n^z\varphi_n^{\pm} = \pm\tfrac{1}{2}\varphi_n^{\pm} \tag{15}$$

where $n = \mathrm{A}$ or B. Using (12) and (15) we get

$$\mathbf{H}_{eff} = \frac{X+Y}{2} + 2\sum_{\mu} J_\mu S_A^\mu S_B^\mu + 2\sum_{\mu\nu} D_{\mu\nu} S_A^\mu S_B^\nu + \mathbf{A}(\boldsymbol{S}_A \times \boldsymbol{S}_B) \tag{16}$$

where $\mu = x, y$ or z. The exchange parameters J_μ, $D_{\mu\nu}$ and $\mathbf{A}$ are expressed through matrix elements of the 4×4 matrix (12)

$$\begin{aligned}
&J_x = (a + a^* + b + b^*)/2 \qquad D_{xy} = D_{yx} = \mathrm{i}(a - a^*)/2\\
&J_y = (-a - a^* + b + b^*)/2 \qquad D_{yz} = D_{zy} = \mathrm{i}(c - c^* + d - d^*)/2\\
&J_z = X - Y \qquad D_{xz} = D_{zx} = (c + c^* + d + d^*)/2\\
&A_x = \mathrm{i}(d - d^* - c + c^*)\\
&A_y = c + c^* - d - d^*\\
&A_z = \mathrm{i}(b^* - b).
\end{aligned} \tag{17}$$

Note that, according to (15), the quantization axes x, y and z for each ion are determined by the choice of the wavefunctions $\varphi_A^{\mp}$ and $\varphi_B^{\mp}$ of components of Kramers doublets. This choice should relate the effective spin to the magnetic moment of the lanthanide ion, so it depends on the specific CF symmetry and orientations of the principal axes of g-tensors of lanthanide ions A and B. In the general case, this problem is rather complicated (especially for low CF symmetries) and is not discussed here. Below in this paper we deal only with cubic symmetry of the CF potential, for which the g-tensor of the ground Kramers doublet is isotropic and the magnetic moment of the lanthanide ion is simply proportional to the effective spin $S = \frac{1}{2}$. In this case the initial choice of the quantization axes is arbitrary and their final orientation is determined under the condition that the resulting spin Hamiltonian (16) is diagonal in spin components (see section 3.4.1).

2.3. A simple testing system

The efficiency of this approach can be illustrated for the simplest exchange pair of two hydrogen-like atoms. Let each of the ions A and B have only one non-degenerate orbital occupied by one electron, $a(\boldsymbol{r})$ and $b(\boldsymbol{r})$, respectively. For this system we can simply write $\varphi_A^+ = a(\boldsymbol{r})\alpha$, $\varphi_A^- = a(\boldsymbol{r})\beta$, $\varphi_B^+ = b(\boldsymbol{r})\alpha$ and $\varphi_B^- = b(\boldsymbol{r})\beta$ for the wavefunctions of the Kramers doublets, so the antisymmetrized two-ion wavefunctions (11) of the ground level are

$$\varphi_A^+\varphi_B^+ = \frac{1}{\sqrt{2}}[a(\boldsymbol{r}_1)b(\boldsymbol{r}_2) - a(\boldsymbol{r}_2)b(\boldsymbol{r}_1)]\alpha_1\alpha_2$$

$$\varphi_A^-\varphi_B^- = \frac{1}{\sqrt{2}}[(a(\boldsymbol{r}_1)b(\boldsymbol{r}_2) - a(\boldsymbol{r}_2)b(\boldsymbol{r}_1)]\beta_1\beta_2$$
$$\varphi_A^+\varphi_B^- = \frac{1}{\sqrt{2}}[a(\boldsymbol{r}_1)b(\boldsymbol{r}_2)\alpha_1\beta_2 - a(\boldsymbol{r}_2)b(\boldsymbol{r}_1)\alpha_2\beta_1]$$
$$\varphi_A^-\varphi_B^+ = \frac{1}{\sqrt{2}}[a(\boldsymbol{r}_1)b(\boldsymbol{r}_2)\beta_1\alpha_2 - a(\boldsymbol{r}_2)b(\boldsymbol{r}_1)\beta_2\alpha_1] \tag{18}$$

where $\boldsymbol{r}_n$ and $\alpha_n = |\frac{1}{2}\rangle$, $\beta_n = |-\frac{1}{2}\rangle$ are, respectively, coordinates and spin eigenfunctions of the nth electron ($n = 1$ and 2).

There are only two wavefunctions $Q_{mn}(\mathrm{B} \to \mathrm{A})$ and $Q_{mn}(\mathrm{A} \to \mathrm{B})$ referring to the 'ionic' states $\mathrm{A}^-\mathrm{B}^+$ and $\mathrm{A}^+\mathrm{B}^-$, in which two electrons are paired on ions A and B, respectively,

$$Q(\mathrm{B} \to \mathrm{A}) = \frac{1}{\sqrt{2}}a(\boldsymbol{r}_1)a(\boldsymbol{r}_2)(\alpha_1\beta_2 - \alpha_2\beta_1)$$
$$Q(\mathrm{A} \to \mathrm{B}) = \frac{1}{\sqrt{2}}b(\boldsymbol{r}_1)b(\boldsymbol{r}_2)(\alpha_1\beta_2 - \alpha_2\beta_1). \tag{19}$$

The energies of these states are U_B and U_A, respectively (which are often referred to as Hubbard energies, describing repulsion between two electrons on the same ion). Matrix elements $\langle\varphi_A^{\pm}\varphi_B^{\pm}|\mathbf{H}_{AB}|Q(\mathrm{A} \to \mathrm{B})\rangle$ are easily expressed in terms of the transfer integral $t = \langle a|\mathbf{h}_{AB}|b\rangle$ (table 1). Using (14) we have

$$X = a = c = d = 0 \qquad Y = -t^2\left(\frac{1}{U_A} + \frac{1}{U_B}\right) \qquad b = t^2\left(\frac{1}{U_A} + \frac{1}{U_B}\right). \tag{20}$$

Finally, using (17), we find

$$J_x = J_y = J_z = t^2\left(\frac{1}{U_A} + \frac{1}{U_B}\right) \qquad \frac{X+Y}{2} = -\frac{t^2}{2}\left(\frac{1}{U_A} + \frac{1}{U_B}\right)$$
$$D_{xy} = D_{yz} = D_{xz} = 0 \qquad A_x = A_y = A_z = 0.$$

That is we obtain the usual antiferromagnetic Heisenberg spin Hamiltonian

$$\mathbf{H}_{eff} = 2t^2\left(\frac{1}{U_A} + \frac{1}{U_B}\right)(-\tfrac{1}{4} + \boldsymbol{S}_A \cdot \boldsymbol{S}_B) \tag{21}$$

as it should be for two exchange-coupled hydrogen-like atoms. In the particular case of $U_A = U_B = U$ we have

$$\mathbf{H}_{eff} = -\frac{t^2}{U} + \frac{4t^2}{U}\boldsymbol{S}_A \cdot \boldsymbol{S}_B. \tag{22}$$

This result coincides with that obtained in [10, 11].

Table 1. $\langle\varphi_A^{\pm}\varphi_B^{\pm}|\mathbf{H}_{AB}|Q_{mn}(\mathrm{A} \leftrightarrow \mathrm{B})\rangle$ matrix elements for the exchange pair of hydrogen-like atoms.

$Q_{mn}(\mathrm{A} \leftrightarrow \mathrm{B})$ charge transfer states	Ground state			
	$\varphi_A^+\varphi_B^+$	$\varphi_A^-\varphi_B^-$	$\varphi_A^+\varphi_B^-$	$\varphi_A^-\varphi_B^+$
$\mathrm{A} \to \mathrm{B}$	0	0	t	$-t$
$\mathrm{B} \to \mathrm{A}$	0	0	t	$-t$

2.4. Bridging ligands, transfer integrals and superexchange pathways

In this section we develop a microscopic model to relate the transfer integrals t_{ij} (which are one-electron matrix elements of the perturbation Hamiltonian $\mathbf{H}_{AB}$ (4)) to the geometry of the exchange pair and the electronic structure of magnetic ions and bridging ligands. For two ions in direct contact with each other, the transfer integrals t_{ij} coincide with the conventional resonance integrals ε_{ij}, which connect atomic orbitals ψ_i and ϕ_j referring to different ions,

$$t_{ij} = \varepsilon_{ij} = \int \psi_i^* \left(\frac{\boldsymbol{p}^2}{2m} + V(\boldsymbol{r}) \right) \phi_j \, \mathrm{d}\boldsymbol{r}. \tag{23}$$

These values are common to quantum chemistry calculations and can be evaluated by various methods. In particular, they can be computed from first principles or obtained using different empirical methods such as the Wolfsberg–Helmholz approximation

$$\varepsilon_{ij} = \frac{K}{2}(E(\psi_i) + E(\phi_j))S_{ij} \tag{24}$$

where $E(\psi_i)$ and $E(\phi_j)$ are the corresponding orbital energies, S_{ij} is the overlap integral between the ψ_i and ϕ_j orbitals, and K is an empirical constant [21].

This problem is considerably complicated when going from a two-centre system to a three-centre system like the lanthanide exchange pair Ln^{3+}(A)–Ligand–Ln^{3+}(B). In such a system, electrons cannot transfer from ion A to ion B by passing through the bridging ligand directly, because 4f atomic orbitals of different lanthanide ions overlap only with the ns and np valent orbitals of the ligand, whereas their direct overlap is negligible. As a consequence, the $\mathrm{Ln}^{3+}(\mathrm{A}) \to \mathrm{Ln}^{3+}(\mathrm{B})$ electron transfer process goes in two steps through intermediate ionized states of the ligands. The general scheme of this virtual process is shown in figure 2. Since typical ligands (such as F^-, O^{2-}, Cl^- and S^{2-}) have a closed electronic $n\mathrm{s}^2 n\mathrm{p}^6$ shell, they cannot accept an extra electron. Instead, in the first step an electron moves from the ligand L to the lanthanide ion B forming the ionized $n\mathrm{s}^1 n\mathrm{p}^6$ or $n\mathrm{s}^2 n\mathrm{p}^5$ configuration to the ligand. In the second step, another electron transfers from the lanthanide ion A to the ligand L, restoring the original $n\mathrm{s}^2 n\mathrm{p}^6$ configuration. The resulting transfer integrals t_{ij} are evaluated in second-order perturbation through resonance integrals and energies of electron transfer from the ligand to the lanthanide ion, $\Delta E_{ik}(\mathrm{L} \to \mathrm{Ln}^{3+})$,

$$t_{ij} = -\sum_{k \in n\mathrm{s}, n\mathrm{p}} \frac{\varepsilon_{ik}(\mathrm{L} \to \mathrm{B})\varepsilon_{kj}(\mathrm{A} \to \mathrm{L})}{\Delta E_{ik}(\mathrm{L} \to \mathrm{Ln}^{3+})}. \tag{25}$$

This procedure is quite valid for lanthanide systems, in which the ligand–metal charge-transfer energy $\Delta E_{ik}(\mathrm{L} \to \mathrm{Ln}^{3+})$ is normally much larger than the corresponding resonance integrals, $\varepsilon_{ik}(\mathrm{L} \to \mathrm{A})$ and $\varepsilon_{kj}(\mathrm{L} \to \mathrm{B})$.

This model is not in conflict with the general approach developed in section 2.2, in which all of the ligand's orbitals are regarded as completely occupied and ligand electrons are not considered. Indeed, in the scheme shown in figure 2 the number of electrons on ligands is changed only in intermediate states, whereas all initial and final states have closed electronic shells on ligands. This means that A–L–B $\to$ A–L^+–B^- $\to$ A^+–L–B^- processes are transformed to direct transitions AB $\to$ $\mathrm{A}^+\mathrm{B}^-$ upon the projection $\mathbf{H} \to \mathbf{H}_1$ described in section 2.2.

If there is more than one bridging ligand $\mathrm{L}_1, \ldots, \mathrm{L}_q$, then equation (25) is generalized by

$$t_{ij} = -\sum_{q}^{ligands} \sum_{k \in n\mathrm{s}, n\mathrm{p}} \frac{\varepsilon_{ik}(\mathrm{L}_q \to \mathrm{B})\varepsilon_{kj}(\mathrm{A} \to \mathrm{L}_q)}{\Delta E_{ik}(\mathrm{L}_q \to \mathrm{Ln}^{3+})}. \tag{26}$$

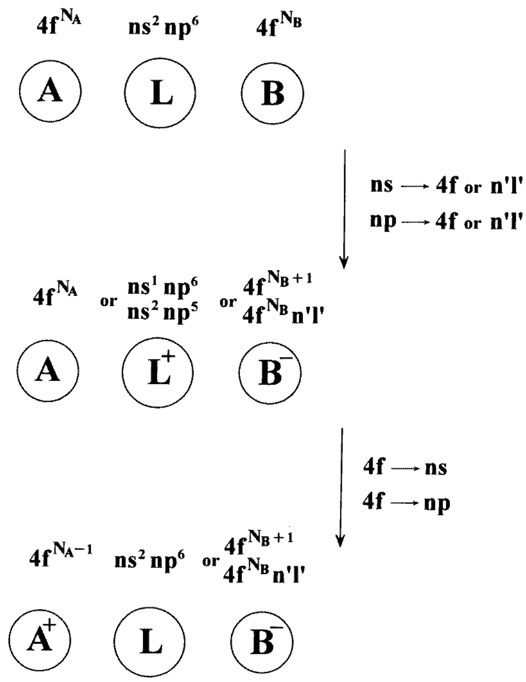

Figure 2. The general scheme of electron transfer processes in the Ln^{3+}(A)–L–Ln^{3+}(B) exchange pair.

Each term in (26) corresponds to a certain electron transfer pathway. Note that the resulting transfer integrals t_{ij} (26) are additive for different pathways which involve different ligands and different combinations of the initial, intermediate and final orbitals, $i \in Ln^{3+}(A)$, $k \in L_q$ and $j \in Ln^{3+}(B)$. However, this is not true for the resulting exchange parameters J_μ, $D_{\mu\nu}$ and A in the spin Hamiltonian (16), because contributions resulting from different exchange pathways can differ both in magnitude and in sign, so some interference effects are possible in the superexchange mechanism for ion pairs involving several bridging ligands. Some of these effects were discussed earlier in [15, 16]. Note that our approach is more general because equation (26) in combination with relations (14) describes all possible electron transfer mechanisms in the M(A)–(L_1, L_2, ... L_n)–M(B) exchange system involving so-called 'ring exchange' and related processes [15, 16, 22].

Although this model is by no means a quantitative solution of the problem with the transfer integrals, it nonetheless gives a useful background for a consistent analysis of microscopic mechanisms of virtual transfers of electrons between magnetic ions via intermediate-valent orbitals of ligands and allows evaluation of transfer integrals t_{ij} in terms of such quantum-mechanical quantities as overlap integrals and orbital energies. In section 3 this model is used for the M_2L_{10} and M_2L_{11} f^1–f^1 dimers to select electron transfer pathways giving non-vanishing contributions to the spin Hamiltonian and to calculate transfer integrals.

3. Mechanisms of f^1–f^1 superexchange interactions

Application of this superexchange theory to actual lanthanide compounds has the difficulty that a large number of excited charge-transfer states $Q_{mn}(A \rightarrow B)$ are involved in calculations. For instance, for $4f^3$–$4f^3 \rightarrow 4f^2$–$4f^3 5d$ electron transfer processes in a Nd^{3+}–Nd^{3+} pair this number is determined by the product of the numbers of states in the $4f^2$ and $4f^3 5d$ configurations, $91 \times 3640 \approx 300\,000$. This needs, therefore, numerical calculations.

In this paper we concentrate on the simplest case of an f^1–f^1 exchange pair, for which an analytical study is still possible due to the comparatively small number of $Q_{mn}(A \leftrightarrow B)$ states. We consider M_2L_{10} and M_2L_{11} dimers involving two equivalent lanthanide or actinide ions M of f^1 configuration (such as Ce^{3+}, Pr^{4+}, U^{5+} or Np^{6+}). Each ion M is surrounded by six ligands L forming a regular octahedron ML_6 (figure 1). These dimers correspond, respectively, to the 90° and 180° geometries of the M–L–M bridging groups, and they serve as idealized models of exchange pairs in cubic crystals. In particular, the 90° geometry occurs for nearest cations in the rock-salt-type structure and the 180° geometry is typical of many cubic crystals, such as perovskites.

3.1. The ground electronic state of f^1 ions

The ground state of an f^1 ion in an octahedral ligand environment is a $\Gamma_7^{(1)}$ Kramers doublet originating from the CF splitting of the lower $^2F_{5/2}$ manifold [23] (figure 3):

$$|\Gamma_{7'}^{(1)}\pm\rangle = \frac{1}{\sqrt{6}}[|\pm\tfrac{5}{2}\rangle - \sqrt{5}|\mp\tfrac{3}{2}\rangle]. \tag{27}$$

Wavefunctions $\varphi^{\pm} = |\Gamma_{7'}^{(1)}\pm\rangle$ can be expressed through f orbitals (f_m orbitals in the $|lm\rangle$ representation or f orbitals of the cubic basis set):

$$\begin{aligned}
\varphi^+ &= \frac{1}{\sqrt{42}}(\sqrt{6}f_3\beta - f_2\alpha - \sqrt{10}f_{-1}\beta + 5f_{-2}\alpha)\\
&= \frac{1}{\sqrt{21}}(2f_{x(y^2-z^2)}\beta + 2if_{y(z^2-x^2)}\beta - 3if_{xyz}\alpha + 2f_{z(x^2-y^2)}\alpha)\\
\varphi^- &= \frac{1}{\sqrt{42}}(\sqrt{6}f_{-3}\alpha - f_{-2}\beta - \sqrt{10}f_1\alpha + 5f_2\beta)\\
&= \frac{1}{\sqrt{21}}(-2f_{x(y^2-z^2)}\alpha + 2if_{y(z^2-x^2)}\alpha + 3if_{xyz}\beta + 2f_{z(x^2-z^2)}\beta)
\end{aligned} \tag{28}$$

where the x, y and z axes are chosen as shown in figure 1.

In fact, the CF effect mixes wavefunctions of the ground $\Gamma_7^{(1)}$ level and excited $\Gamma_7^{(2)}$ level stemming from the upper $^2F_{7/2}$ manifold which contains f_{x^3}, f_{y^3} and f_{z^3} orbitals (figure 3). This mixing is, however, rather small, even for f^1 systems with strong CF effects, such as UF_6^- and UCl_6^- complexes [24, 25], so it can be neglected to a first approximation.

3.2. Excited charge-transfer states A^+B^- and A^-B^+ of a f^1–f^1 pair

In charge-transfer states A^+B^- of a f^1–f^1 pair ion A has no electrons in the valence shell whereas ion B has two electrons in the $4f^2$ or $4fn'l'$ configuration, $4f^0(A)$–$4f^2(B)$ or $4f^0(A)$–$4f(B)n'l'(B)$ (the same is true for the back transition $AB \rightarrow A^-B^+$). Therefore, charge-transfer functions $Q_{mn}(A \rightarrow B)$ and $Q_{mn}(B \rightarrow A)$ coincide with the usual single-ion wavefunctions of the relevant $4f^2$ or $4fn'l'$ electronic configuration of ions B and A, respectively. Below in this paper we take into account only the 4f5d configuration, which seems to be the most important one for the f^1–f^1 superexchange (contributions of 4f5d and $4f^2$ configurations are compared in section 3.5).

We assume that charge-transfer energies $E_{mn}(A \rightarrow B)$ can be written as $U + E_n(fd)$ where U is a constant and $E_n(fd)$ is the energy of the nth level of the 4f5d configuration

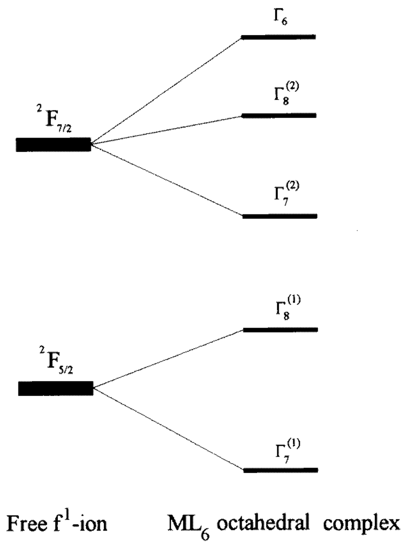

Figure 3. The splitting of energy levels of f^1 ions in an octahedral crystal field.

(in the case of a f^1–f^1 pair, the double index mn in charge-transfer functions $Q_{mn}(A \to B)$ transforms to the single index n because the index m vanishes for the empty $4f^0$ configuration).

The energy structure of the 4f5d configuration of a free lanthanide ion is mainly determined by Coulomb interaction between 4f and 5d electrons, which is described by three Coulomb $F^{2k}(4f, 5d)$ and three exchange $G^{2k+1}(4f, 5d)$ Slater parameters (where $k = 0$, 1 and 2) [26]. The spin–orbit energy for 4f and 5d orbitals is of minor importance. The strong CF effect splits the 5d level into the lower triply degenerate t_{2g} level ($5d_{xy}$, $5d_{yz}$ and $5d_{zx}$ orbitals) and the upper doubly degenerate e_g level ($5d_{z^2}$ and $5d_{x^2-y^2}$ orbitals). In addition, a small CF splitting occurs for 4f states. The energy structure of the 4f5d configuration is therefore rather complicated, so a more simple model has to be used, which, on the one hand, allows an analytical study and, on the other hand, reflects the main features of the energy structure of the 4f5d configuration. This model is based on the following assumptions.

(i) Intra-ionic Coulomb interaction between 4f and 5d electrons is described by one parameter U_{fd} corresponding to the spherical part of the electron–electron repulsion potential $F^0(4f, 5d)$, whereas the non-spherical part ($F^2(4f, 5d)$ and $F^4(4f, 5d)$ parameters) is neglected. In lanthanide ions, this parameter is typically $U_{fd} \approx F^0(4f, 5d) \approx 10$ eV. We also assume that the U_{fd} parameter involves the energy difference between 4f and 5d orbitals and the electron–hole interaction energy g_{AB}.

(ii) Spin–orbit energies of 4f and 5d states as well as the CF splitting energy of the 4f state (≈ 100 cm^{-1}) are neglected.

(iii) The CF splitting $10Dq$ between e_g and t_{2g} 5d levels is taken into account. The CF effect increases the energy of the e_g level by the value $6Dq$ and lowers the energy of the t_{2g} level by $4Dq$. This splitting is normally of order $10Dq \approx 2$–3 eV for Ln^{3+} ions in octahedral environment of six ligands [9].

(iv) Intra-ionic exchange interaction between 4f and 5d electrons is approximated by one effective exchange parameter I_{fd} instead of three exchange parameters $G^{2k+1}(4f, 5d)$

($k = 0$, 1 and 2). In other words, we assume that the energy separation between triplet states

$$^3[\mathrm{f}_l\mathrm{d}_k]S_1(M_s) = \frac{1}{\sqrt{2}}(4\mathrm{f}_l(\boldsymbol{r}_1)5\mathrm{d}_k(\boldsymbol{r}_2) - 4\mathrm{f}_l(\boldsymbol{r}_2)5\mathrm{d}_k(\boldsymbol{r}_1))S_1(M_s) \tag{29}$$

(where $S_1(M_s)$ are triplet and spin functions $S_1(+1) = \alpha_1\alpha_2$, $S_1(0) = (\alpha_1\beta_2 + \alpha_2\beta_1)/\sqrt{2}$ and $S_1(-1) = \beta_1\beta_2$) and the corresponding singlet states

$$^1[\mathrm{f}_l\mathrm{d}_k]S_0 = \frac{1}{\sqrt{2}}(4\mathrm{f}_l(\boldsymbol{r}_1)5\mathrm{d}_k(\boldsymbol{r}_2) + 4\mathrm{f}_l(\boldsymbol{r}_2)5\mathrm{d}_k(\boldsymbol{r}_1))S_0 \tag{30}$$

(where $S_0 = (\alpha_1\beta_2 - \alpha_2\beta_1)/\sqrt{2}$ is the singlet spin function) of the 4f5d configuration are the same for either pair of $4\mathrm{f}_l$ and $5\mathrm{d}_k$ orbitals (where $l = 3, 2, \ldots, -3$ and $k = xy$, yz, zx, z^2 and $x^2 - y^2$) and is equal to I_{fd} which is estimated by $I_{fd} \approx G^1(4\mathrm{f}, 5\mathrm{d}) \approx 1$–2 eV. Wavefunctions $Q_{mn}(\mathrm{A} \to \mathrm{B})$ and the corresponding charge-transfer energies $E_{mn}(\mathrm{A} \leftrightarrow \mathrm{B})$ are listed in table 2.

Table 2. Wavefunctions $Q_{mn}(\mathrm{A} \to \mathrm{B})$ and charge-transfer energies $E_{mn}(\mathrm{A} \to \mathrm{B})$ of the M_2L_{10} and M_2L_{11} f^1–f^1 exchange dimers (4f5d configuration on ion B).

State	Wavefunction	Energy $E_{mn}(\mathrm{A} \to \mathrm{B})$
$\varphi_A^{\pm}\varphi_B^{\pm}$ ground state	$\frac{1}{\sqrt{2}}(\varphi_A^{\pm}(\boldsymbol{r}_1, \sigma_1)\varphi_B^{\pm}(\boldsymbol{r}_2, \sigma_2) - \varphi_A^{\pm}(\boldsymbol{r}_2, \sigma_2)\varphi_B^{\pm}(\boldsymbol{r}_1, \sigma_1))$	0
$^3[\mathrm{f}_l\ \mathrm{d}_k]S_1(M_s)$ triplet states	$\frac{1}{\sqrt{2}}(4\mathrm{f}_l(\boldsymbol{r}_1)5\mathrm{d}_k(\boldsymbol{r}_2) - 4\mathrm{f}_l(\boldsymbol{r}_2)5\mathrm{d}_k(\boldsymbol{r}_1))S_1(M_s)$	$U_{fd} - I_{fd} - 4Dq$ ($k = xy$, yz or zx) $U_{fd} - I_{fd} + 6Dq$ ($k = z^2$ or $x^2 - y^2$)
$^1[\mathrm{f}_l\ \mathrm{d}_k]S_0$ singlet states	$\frac{1}{\sqrt{2}}(4\mathrm{f}_l(\boldsymbol{r}_1)5\mathrm{d}_k(\boldsymbol{r}_2) + 4\mathrm{f}_l(\boldsymbol{r}_2)5\mathrm{d}_k(\boldsymbol{r}_1))S_0$	$U_{fd} - 4Dq$ ($k = xy$, yz or zx) $U_{fd} + 6Dq$ ($k = z^2$ or $x^2 - y^2$)

The following notations are assumed:

$\sigma_n = \pm\frac{1}{2}$
$l = 3, 2, \ldots, -3$; $k = xy$, yz, zx, z^2 or $x^2 - y^2$
$S_1(1) = \alpha_1\alpha_2$, $S_1(0) = (1/\sqrt{2})(\alpha_1\beta_2 + \beta_1\alpha_2)$
$S_1(-1) = \beta_1\beta_2$
$S_0 = (1/\sqrt{2})(\alpha_1\beta_2 - \beta_1\alpha_2)$.

3.3. Electron transfer pathways and transfer integrals in the M_2L_{10} and M_2L_{11} f^1–f^1 dimers

We consider specific pathways of virtual transfers of electrons between 4f orbitals of ion A and 5d orbitals of ion B via bridging ligands L in the M_2L_{10} and M_2L_{11} dimers and evaluate the corresponding $t_{ij}(4\mathrm{f}, 5\mathrm{d})$ transfer integrals. Because only four of the seven f orbitals of the cubic set are involved in the ground state wavefunctions (28), we need to derive transfer integrals between these four 4f orbitals of the ion A (namely, $4\mathrm{f}_{xyz}$, $4\mathrm{f}_{z(x^2-y^2)}$, $4\mathrm{f}_{y(z^2-x^2)}$ and $4\mathrm{f}_{x(y^2-z^2)}$) and five 5d orbitals of the ion B ($5\mathrm{d}_{z^2}$ and $5\mathrm{d}_{x^2-y^2}$ e_g orbitals and $5\mathrm{d}_{xy}$, $5\mathrm{d}_{yz}$ and $5\mathrm{d}_{zx}$ t_{2g} orbitals). To do this, we use equation (26) in which the resonance integrals ε_{ik} between 4f and 5d orbitals of lanthanide ions and ns, np ligand orbitals are evaluated with equation (24). We should therefore consider in detail the overlap between the lanthanide 4f or 5d orbitals and the ligand's valency orbitals in the octahedral species ML_6 (figures 4 and 5). Because of cubic symmetry, there are the following selection rules for non-vanishing overlap integrals.

(i) $4f_{z(x^2-y^2)}$, $4f_{y(z^2-x^2)}$ and $4f_{x(y^2-z^2)}$ orbitals overlap with np orbitals in π-type fashion. This group of overlap integrals is parametrized via one parameter $S_\pi(4f, np) = \langle 4f_{y(z^2-x^2)}|np_y\rangle$.

(ii) $5d_{xy}$, $5d_{yz}$ and $5d_{zx}$ orbitals overlap with np orbitals in π-type fashion (figures 4(a), 4(e) and 5), $S_\pi(5d, np) = \langle 5d_{xy}|np_x\rangle$.

(iii) $5d_{z^2}$ and $5d_{x^2-y^2}$ orbitals overlap both with the np and with the ns orbitals of the ligand in σ-type fashion (figures 4(b)–(d)), $S_\sigma(5d, np) = \langle 5d_{z^2}|np_z\rangle$ and $S_\sigma(5d, ns) = \langle 5d_{z^2}|ns\rangle$.

Using the Wolfsberg–Helmholz approximation (24) with $K = 2$ we can derive the corresponding resonance integrals $\varepsilon_{ik}(4f, np)$ and $\varepsilon_{kj}(5d, np)$ as

$$\begin{aligned}\varepsilon_{ik}(4f, np) &= \langle 4f_i|np_k\rangle[E(4f) + E(np)]\\ \varepsilon_{kj}(5d, np) &= \langle np_k|5d_j\rangle[E(5d) + E(np)]\end{aligned} \tag{31}$$

where $E(4f)$, $E(5d)$ and $E(np)$ are the energies of the corresponding atomic orbitals. Note that none of the 4f orbitals overlap with the ligand's ns orbitals. This means that the ligand's ns orbitals play no part in superexchange pathways and do not contribute to the resulting exchange parameters either in M_2L_{10} or in M_2L_{11} dimers.

Using equations (26) and (31) we can now define the transfer integrals between 4f and 5d orbitals as

$$\begin{aligned}t_{ij}(4f, 5d) &= -\sum_{q}^{ligands}\sum_{k\in np(L_q)}\frac{\varepsilon^*_{ik}(4f, np)\varepsilon_{kj}(5d, np)}{\Delta E(L_q \to Ln^{3+})}\\ &= -\sum_{q}^{ligands}\sum_{k\in np(L_q)}\frac{\langle 4f_i(A)|np_k(L_q)\rangle\langle np_k(L_q)|5d_j(A)\rangle}{\Delta E(L_q \to Ln^{3+})}\\ &\quad\times[E(4f) + E(np)][E(5d) + E(np)]\end{aligned} \tag{32}$$

where ligand–lanthanide electron transfer energies $\Delta E(L_q \to Ln^{3+})$ are assumed to be the same both for $np(L_q) \to 4f(Ln^{3+})$ and for $np(L_q) \to 5d(Ln^{3+})$ transfers. They can be approximated by the difference between the corresponding orbital energies, $\Delta E(L_q \to Ln^{3+}) \approx E(4f) - E(np) \approx E(5d) - E(np)$. In particular, for oxide compounds we have $E(2p) \approx -15$ eV, $E(4f) \approx -7$ eV and $\Delta E(O^{2-} \to Ln^{3+}) \approx 8$ eV. It follows from (32) that the $t_{ij}(4f, 5d)$ transfer integral is only non-vanishing if there is at least one $4f_k(A) \to np_i(L_q) \to 5d_1(B)$ electron transfer pathway, in which the $\langle 4f_i|np_k(L_q)\rangle$ and $\langle np_k(L_q)|5d_j\rangle$ overlap integrals are simultaneously non-zero. This leads to some selection rules for non-vanishing transfer integrals which are different for the 90° and 180° geometries of the exchange pair.

3.3.1. The 90° geometry. Overlap integrals between 4f(A) and 5d(B) lanthanide and $np(L_1)$ and $np(L_2)$ ligand orbitals in the M_2L_{10} dimer expressed in terms of the $S_\pi(4f, np)$, $S_\pi(5d, np)$ and $S_\sigma(5d, np)$ parameters are listed in table 3. Using these values and equation (32), we can determine non-vanishing transfer integrals t_{lk}(4f–5d) through two parameters $T_{\pi\sigma}$ and $T_{\pi\pi}$,

$$T_{\pi\sigma} = -\frac{S_\pi(4f, np)S_\sigma(5d, np)}{\Delta E(L \to Ln^{3+})}[E(4f) + E(np)][E(5d) + E(np)] \tag{33a}$$

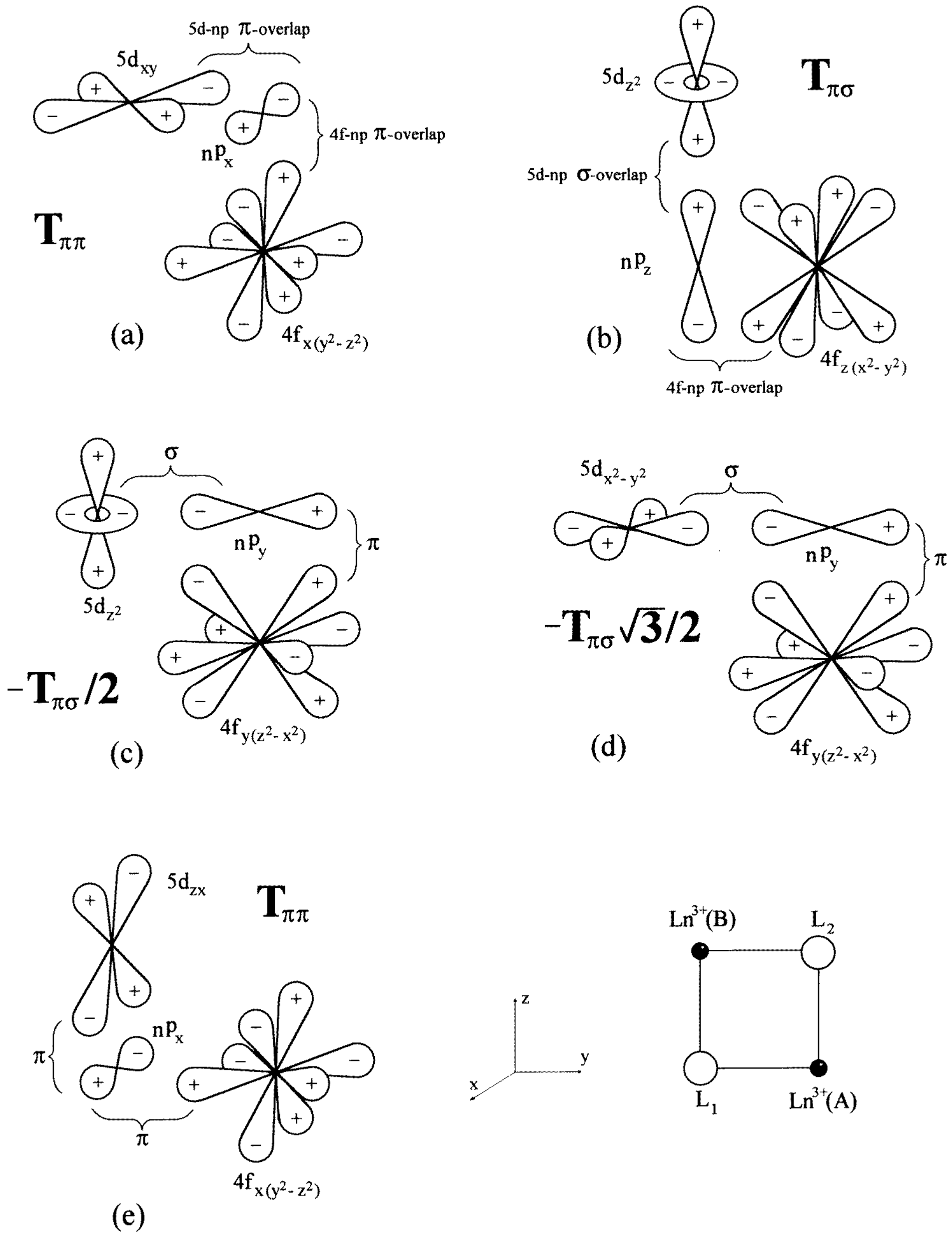

Figure 4. Electron transfer pathways and overlaps of 4f and 5d lanthanide orbitals and ns and np valency orbitals of the bridging ligands in the M_2L_{10} f^1–f^1 dimer. The cases (a) and (e) correspond to electron transfer pathways 4f(A) $\rightarrow$ np(L) $\rightarrow$ 5d(B) of $\pi\pi$ type, whereas cases (b), (c) and (d) correspond to $\pi\sigma$ pathways (the resulting transfer integral $t_{ij}(4\mathrm{f}, 5\mathrm{d})$ of each pathway is shown in the corresponding picture).

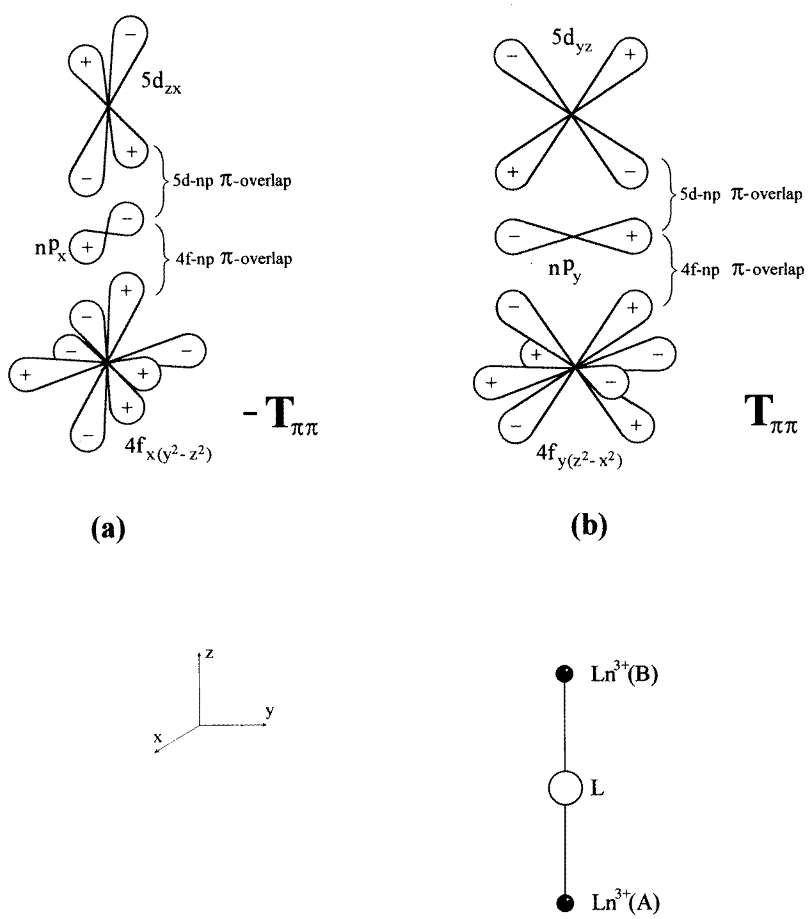

Figure 5. Electron transfer pathways and overlaps of 4f and 5d lanthanide orbitals and ns and np valency orbitals of the bridging ligands in the M_2L_{11} f^1–f^1 dimer. Two $\pi\pi$ pathways are shown which have non-vanishing transfer integrals.

$$T_{\pi\pi} = -\frac{S_\pi(4\text{f}, n\text{p})S_\pi(5\text{d}, n\text{p})}{\Delta E(\text{L} \rightarrow \text{Ln}^{3+})}[E(4\text{f}) + E(n\text{p})][E(5\text{d}) + E(n\text{p})]. \qquad (33b)$$

The $T_{\pi\sigma}$ parameter corresponds to the electron transfer pathway in which the 4f(A) orbital overlaps with the np(L) orbital in π-type fashion, whereas 5d(B) and np(L) orbitals overlap in σ-type fashion as is the case for the $4\text{f(A)}_{z(x^2-y^2)} \rightarrow n\text{p}_z(\text{L}_1) \rightarrow 5\text{d(B)}_{z^2}$ pathway (figure 4(b)). Similarly, the $T_{\pi\pi}$ parameter refers to a pathway in which both 4f(A) and 5d(B) orbitals overlap with the intermediate ligand's np(L) orbitals in π-type fashion, as is the case for the $4\text{f(A)}_{x(y^2-z^2)} \rightarrow n\text{p}_x(\text{L}_2) \rightarrow 5\text{d(B)}_{xy}$ pathway (figure 4(a)). The corresponding transfer integrals are given in table 4 and all electron transfer pathways resulting in non-vanishing transfer integrals are shown in figures 4(a)–(e).

3.3.2. The 180° geometry. There are only two pathways in the M_2L_{11} dimer (both of $\pi\pi$ type), $4\text{f(A)}_{x(y^2-z^2)} \rightarrow n\text{p}_x(\text{L}) \rightarrow 5\text{d(B)}_{zx}$ and $4\text{f(A)}_{y(z^2-x^2)} \rightarrow n\text{p}_y(\text{L}) \rightarrow 5\text{d(B)}_{yz}$ (figures 5(a) and (b)). As a result, 4f–5d transfer integrals are expressed only via one parameter, $T_{\pi\pi}$ (33b) (table 5).

Table 3. Overlap integrals between 4f and 5f metal orbitals and ns and np valent orbitals of the bridging ligands in the M_2L_{10} dimer.

Metal orbitals	Ligand orbitals							
	$n\mathrm{p}_x$ (L_1)	$n\mathrm{p}_y$ (L_1)	$n\mathrm{p}_z$ (L_1)	$n\mathrm{p}_x$ (L_2)	$n\mathrm{p}_y$ (L_2)	$n\mathrm{p}_z$ (L_2)	ns (L_1)	ns (L_2)
$4\mathrm{f}_{xyz}$(A)	0	0	0	0	0	0	0	0
$4\mathrm{f}_{x(y^2-z^2)}$(A)	S_π(4f, np)	0	0	$-S_\pi$(4f, np)	0	0	0	0
$4\mathrm{f}_{y(z^2-x^2)}$(A)	0	0	0	0	S_π(4f, np)	0	0	0
$4\mathrm{f}_{z(x^2-y^2)}$(A)	0	0	$-S_\pi$(4f, np)	0	0	0	0	0
$5\mathrm{d}_{xy}$(B)	0	0	0	S_π(5d, np)	0	0	0	0
$5\mathrm{d}_{yz}$(B)	0	$-S_\pi$(5d, np)	0	0	0	S_π(5d, np)	0	0
$5\mathrm{d}_{zx}$(B)	$-S_\pi$(5d, np)	0	0	0	0	0	0	0
$5\mathrm{d}_{z^2}$(B)	0	0	S_σ(5d, np)	0	$S_\sigma(5\mathrm{d}, n\mathrm{p})/2$	0	S_σ(5d, ns)	$-S_\sigma(5\mathrm{d}, n\mathrm{p})/2$
$5\mathrm{d}_{x^2-y^2}$(B)	0	0	0	0	$S_\sigma(5\mathrm{d}, n\mathrm{p})\sqrt{3}/2$	0	0	$-S_\sigma(5\mathrm{d}, n\mathrm{s})\sqrt{3}/2$

Table 4. t_{ij}(4f, 5d) transfer integrals in the M_2L_{10} dimer.

$5d_i$(B) orbitals	$4f_j$(A) orbitals[a]			
	$4f_{xyz}$	$4f_{x(y^2-z^2)}$	$4f_{y(z^2-x^2)}$	$4f_{z(x^2-y^2)}$
$5d_{xy}$	0	$T_{\pi\pi}$ (L$_2$)	0	0
$5d_{yz}$	0	0	0	0
$5d_{zx}$	0	$T_{\pi\pi}$ (L$_1$)	0	0
$5d_{z^2}$	0	0	$-T_{\pi\sigma}/2$ (L$_2$)	$T_{\pi\sigma}$ (L$_1$)
$5d_{x^2-y^2}$	0	0	$-T_{\pi\sigma}\sqrt{3}/2$ (L$_2$)	0

[a] The ligand contributing to the corresponding non-vanishing transfer integral is indicated in parentheses.

Table 5. t_{ij}(4f, 5d) transfer integrals in the M_2L_{11} dimer.

$5d_i$(B) orbitals	$4f_j$(A) orbitals			
	$4f_{xyz}$	$4f_{x(y^2-z^2)}$	$4f_{y(z^2-x^2)}$	$4f_{z(x^2-y^2)}$
$5d_{xy}$	0	0	0	0
$5d_{yz}$	0	0	$T_{\pi\pi}$	0
$5d_{zx}$	0	$-T_{\pi\pi}$	0	0
$5d_{z^2}$	0	0	0	0
$5d_{x^2-y^2}$	0	0	0	0

3.4. *Effective spin Hamiltonians of the f^1–f^1 superexchange*

Based on the above results we now derive effective spin Hamiltonians for the M_2L_{10} and M_2L_{11} f^1–f^1 exchange dimers. Using the $Q_{mn}(A \to B)$ charge transfer wavefunctions from table 2 we first calculate $\langle \varphi_A^{\pm}\varphi_B^{\pm}|\mathbf{H}_{AB}|Q_{mn}(A \to B)\rangle$ two-ion matrix elements and then derive the exchange parameters J_μ, D_{mv} and $\mathbf{A}$ using charge transfer energies $E_{mn}(A \to B)$ from table 2 and equations (14)–(17). Because ions A and B are equivalent, we take into account A^+B^- states only and then multiply the result by a factor of two. Details of calculation of the $\langle \varphi_A^{\pm}\varphi_B^{\pm}|\mathbf{H}_{AB}|Q_{mn}(A \to B)\rangle$ matrix elements are presented in the appendix.

3.4.1. Spin Hamiltonian of the M_2L_{10} dimer. Using the $Q_{mn}(A \to B)$ wavefunctions from table 2 and transfer integrals from table 4, we calculate matrix elements $\langle \varphi_A^{\pm}\varphi_B^{\pm}|\mathbf{H}_{AB}|Q_{mn}(A \to B)\rangle$ for the M_2L_{10} dimer (table 6). Replacing these matrix elements into (14), we calculate the matrix elements X, Y, a, b, c and d of the effective exchange Hamiltonian $\mathbf{H}_{eff}$ (12) summing over 140 $Q_{mn}(A \to B)$ states of the 4f5d configuration:

$$X = -\frac{4T_{\pi\sigma}^2}{21}\left(\frac{3}{U_{fd} - I_{fd} + 6Dq} + \frac{1}{U_{fd} + 6Dq}\right) - \frac{8T_{\pi\pi}^2}{441}\left(\frac{29}{U_{fd} - I_{fd} - 4Dq} + \frac{13}{U_{fd} - 4Dq}\right)$$

$$Y = -\frac{4T_{\pi\sigma}^2}{21}\left(\frac{3}{U_{fd} - I_{fd} + 6Dq} + \frac{1}{U_{fd} + 6Dq}\right) - \frac{8T_{\pi\pi}^2}{441}\left(\frac{34}{U_{fd} - I_{fd} - 4Dq} + \frac{8}{U_{fd} - 4Dq}\right)$$

Table 6. $\langle\varphi_A^{\pm}\varphi_B^{\pm}|\mathbf{H}_{AB}|Q_{mn}(\mathrm{A}\to\mathrm{B})\rangle$ two-ion matrix elements for the M_2L_{10} dimer.

$Q_{mn}(\mathrm{A}\to\mathrm{B})$ charge transfer states	Ground state			
	$\varphi_A^+\varphi_B^+$	$\varphi_A^-\varphi_B^-$	$\varphi_A^+\varphi_B^-$	$\varphi_A^-\varphi_B^+$
$^3[f_3\, d_{xy}]S_1(1)$	0	0	0	0
$^3[f_2\, d_{xy}]S_1(1)$	0	0	0	$-T_{\pi\pi}\sqrt{2/21}$
$^3[f_1\, d_{xy}]S_1(1)$	0	$T_{\pi\pi}\sqrt{12/21}$	0	0
$^3[f_0\, d_{xy}]S_1(1)$	0	0	0	0
$^3[f_{-1}\, d_{xy}]S_1(1)$	0	0	0	0
$^3[f_{-2}\, d_{xy}]S_1(1)$	0	0	0	$T_{\pi\pi}\sqrt{50/21}$
$^3[f_{-3}\, d_{xy}]S_1(1)$	0	$-T_{\pi\pi}\sqrt{20/21}$	0	0
$^3[f_3\, d_{xy}]S_1(0)$	0	0	0	$T_{\pi\pi}\sqrt{6/21}$
$^3[f_2\, d_{xy}]S_1(0)$	$T_{\pi\pi}/21$	$T_{\pi\pi}5/21$	0	0
$^3[f_1\, d_{xy}]S_1(0)$	0	0	$T_{\pi\pi}\sqrt{10/21}$	0
$^3[f_0\, d_{xy}]S_1(0)$	0	0	0	0
$^3[f_{-1}\, d_{xy}]S_1(0)$	0	0	0	$-T_{\pi\pi}\sqrt{10/21}$
$^3[f_{-2}\, d_{xy}]S_1(0)$	$-T_{\pi\pi}5/21$	$-T_{\pi\pi}/21$	0	0
$^3[f_{-3}\, d_{xy}]S_1(0)$	0	0	$-T_{\pi\pi}\sqrt{6/21}$	0
$^3[f_3\, d_{xy}]S_1(-1)$	$-T_{\pi\pi}\sqrt{12/21}$	0	0	0
$^3[f_2\, d_{xy}]S_1(-1)$	0	0	$-T_{\pi\pi}\sqrt{50/21}$	0
$^3[f_1\, d_{xy}]S_1(-1)$	0	0	0	0
$^3[f_0\, d_{xy}]S_1(-1)$	0	0	0	0
$^3[f_{-1}\, d_{xy}]S_1(-1)$	$T_{\pi\pi}\sqrt{20/21}$	0	0	0
$^3[f_{-2}\, d_{xy}]S_1(-1)$	0	0	$T_{\pi\pi}\sqrt{2/21}$	0
$^3[f_{-3}\, d_{xy}]S_1(-1)$	0	0	0	0
$^1[f_3\, d_{xy}]S_0$	0	0	0	$-T_{\pi\pi}\sqrt{6/21}$
$^1[f_2\, d_{xy}]S_0$	$T_{\pi\pi}/21$	$-T_{\pi\pi}5/21$	0	0
$^1[f_1\, d_{xy}]S_0$	0	0	$T_{\pi\pi}\sqrt{10/21}$	0
$^1[f_0\, d_{xy}]S_0$	0	0	0	0
$^1[f_{-1}\, d_{xy}]S_0$	0	0	0	$T_{\pi\pi}\sqrt{10/21}$
$^1[f_{-2}\, d_{xy}]S_0$	$-T_{\pi\pi}5/21$	$T_{\pi\pi}/21$	0	0
$^1[f_{-3}\, d_{xy}]S_0$	0	0	$-T_{\pi\pi}\sqrt{6/21}$	0
$^3[f_3\, d_{zx}]S_1(1)$	0	0	0	0
$^3[f_2\, d_{zx}]S_1(1)$	0	0	0	$-T_{\pi\pi}\sqrt{2/21}$
$^3[f_1\, d_{zx}]S_1(1)$	0	$T_{\pi\pi}\sqrt{12/21}$	0	0
$^3[f_0\, d_{zx}]S_1(1)$	0	0	0	0
$^3[f_{-1}\, d_{zx}]S_1(1)$	0	0	0	0
$^3[f_{-2}\, d_{zx}]S_1(1)$	0	0	0	$T_{\pi\pi}\sqrt{50/21}$
$^3[f_{-3}\, d_{zx}]S_1(1)$	0	$-T_{\pi\pi}\sqrt{20/21}$	0	0
$^3[f_3\, d_{zx}]S_1(0)$	0	0	0	$T_{\pi\pi}\sqrt{6/21}$
$^3[f_2\, d_{zx}]S_1(0)$	$T_{\pi\pi}/21$	$T_{\pi\pi}5/21$	0	0
$^3[f_1\, d_{zx}]S_1(0)$	0	0	$T_{\pi\pi}\sqrt{10/21}$	0
$^3[f_0\, d_{zx}]S_1(0)$	0	0	0	0
$^3[f_{-1}\, d_{zx}]S_1(0)$	0	0	0	$-T_{\pi\pi}\sqrt{10/21}$
$^3[f_{-2}\, d_{zx}]S_1(0)$	$-T_{\pi\pi}5/21$	$-T_{\pi\pi}/21$	0	0
$^3[f_{-3}\, d_{zx}]S_1(0)$	0	0	$-T_{\pi\pi}\sqrt{6/21}$	0
$^3[f_3\, d_{zx}]S_1(-1)$	$-T_{\pi\pi}\sqrt{12/21}$	0	0	0
$^3[f_2\, d_{zx}]S_1(-1)$	0	0	$-T_{\pi\pi}\sqrt{50/21}$	0
$^3[f_1\, d_{zx}]S_1(-1)$	0	0	0	0

Table 6. (Continued)

$Q_{mn}(\mathrm{A} \to \mathrm{B})$ charge transfer states	Ground state			
	$\varphi_A^+\varphi_B^+$	$\varphi_A^-\varphi_B^-$	$\varphi_A^+\varphi_B^-$	$\varphi_A^-\varphi_B^+$
$^3[\mathrm{f}_0\,\mathrm{d}_{zx}]S_1(-1)$	0	0	0	0
$^3[\mathrm{f}_{-1}\,\mathrm{d}_{zx}]S_1(-1)$	$T_{\pi\pi}\sqrt{20/21}$	0	0	0
$^3[\mathrm{f}_{-2}\,\mathrm{d}_{zx}]S_1(-1)$	0	0	$T_{\pi\pi}\sqrt{2/21}$	0
$^3[\mathrm{f}_{-3}\,\mathrm{d}_{zx}]S_1(-1)$	0	0	0	0
$^1[\mathrm{f}_3\,\mathrm{d}_{zx}]S_0$	0	0	0	$-T_{\pi\pi}\sqrt{6/21}$
$^1[\mathrm{f}_2\,\mathrm{d}_{zx}]S_0$	$T_{\pi\pi}/21$	$-T_{\pi\pi}5/21$	0	0
$^1[\mathrm{f}_1\,\mathrm{d}_{zx}]S_0$	0	0	$T_{\pi\pi}\sqrt{10/21}$	0
$^1[\mathrm{f}_0\,\mathrm{d}_{zx}]S_0$	0	0	0	0
$^1[\mathrm{f}_{-1}\,\mathrm{d}_{zx}]S_0$	0	0	0	$T_{\pi\pi}\sqrt{10/21}$
$^1[\mathrm{f}_{-2}\,\mathrm{d}_{zx}]S_0$	$-T_{\pi\pi}5/21$	$T_{\pi\pi}/21$	0	0
$^1[\mathrm{f}_{-3}\,\mathrm{d}_{zx}]S_0$	0	0	$-T_{\pi\pi}\sqrt{6/21}$	0
$^3[\mathrm{f}_3\,\mathrm{d}_{z^2}]S_1(1)$	0	0	0	0
$^3[\mathrm{f}_2\,\mathrm{d}_{z^2}]S_1(1)$	$T_{\pi\sigma}\sqrt{2/21}$	0	0	$-\mathrm{i}T_{\pi\sigma}\sqrt{2/42}$
$^3[\mathrm{f}_1\,\mathrm{d}_{z^2}]S_1(1)$	0	$-\mathrm{i}T_{\pi\sigma}\sqrt{20/42}$	$T_{\pi\sigma}\sqrt{20/21}$	0
$^3[\mathrm{f}_0\,\mathrm{d}_{z^2}]S_1(1)$	0	0	0	0
$^3[\mathrm{f}_{-1}\,\mathrm{d}_{z^2}]S_1(1)$	0	0	0	0
$^3[\mathrm{f}_{-2}\,\mathrm{d}_{z^2}]S_1(1)$	$-T_{\pi\sigma}\sqrt{50/21}$	0	0	$\mathrm{i}T_{\pi\sigma}\sqrt{50/42}$
$^3[\mathrm{f}_{-3}\,\mathrm{d}_{z^2}]S_1(1)$	0	$\mathrm{i}T_{\pi\sigma}\sqrt{12/42}$	$-T_{\pi\sigma}\sqrt{12/21}$	0
$^3[\mathrm{f}_3\,\mathrm{d}_{z^2}]S_1(0)$	$-T_{\pi\sigma}\sqrt{6/21}$	0	0	$\mathrm{i}T_{\pi\sigma}\sqrt{6/42}$
$^3[\mathrm{f}_2\,\mathrm{d}_{z^2}]S_1(0)$	$-\mathrm{i}T_{\pi\sigma}/42$	$\mathrm{i}T_{\pi\sigma}5/42$	$-T_{\pi\sigma}5/21$	$T_{\pi\sigma}/21$
$^3[\mathrm{f}_1\,\mathrm{d}_{z^2}]S_1(0)$	0	$T_{\pi\sigma}\sqrt{10/21}$	$-\mathrm{i}T_{\pi\sigma}\sqrt{10/42}$	0
$^3[\mathrm{f}_0\,\mathrm{d}_{z^2}]S_1(0)$	0	0	0	0
$^3[\mathrm{f}_{-1}\,\mathrm{d}_{z^2}]S_1(0)$	$T_{\pi\sigma}\sqrt{10/21}$	0	0	$-\mathrm{i}T_{\pi\sigma}\sqrt{10/42}$
$^3[\mathrm{f}_{-2}\,\mathrm{d}_{z^2}]S_1(0)$	$\mathrm{i}T_{\pi\sigma}5/42$	$-\mathrm{i}T_{\pi\sigma}/42$	$T_{\pi\sigma}/21$	$-T_{\pi\sigma}5/21$
$^3[\mathrm{f}_{-3}\,\mathrm{d}_{z^2}]S_1(0)$	0	$-T_{\pi\sigma}\sqrt{6/21}$	$\mathrm{i}T_{\pi\sigma}\sqrt{6/42}$	0
$^3[\mathrm{f}_3\,\mathrm{d}_{z^2}]S_1(-1)$	$\mathrm{i}T_{\pi\sigma}\sqrt{12/42}$	0	0	$-T_{\pi\sigma}\sqrt{12/21}$
$^3[\mathrm{f}_2\,\mathrm{d}_{z^2}]S_1(-1)$	0	$-T_{\pi\sigma}\sqrt{50/21}$	$\mathrm{i}T_{\pi\sigma}\sqrt{50/42}$	0
$^3[\mathrm{f}_1\,\mathrm{d}_{z^2}]S_1(-1)$	0	0	0	0
$^3[\mathrm{f}_0\,\mathrm{d}_{z^2}]S_1(-1)$	0	0	0	0
$^3[\mathrm{f}_{-1}\,\mathrm{d}_{z^2}]S_1(-1)$	$-\mathrm{i}T_{\pi\sigma}\sqrt{20/42}$	0	0	$T_{\pi\sigma}\sqrt{20/21}$
$^3[\mathrm{f}_{-2}\,\mathrm{d}_{z^2}]S_1(-1)$	0	$T_{\pi\sigma}\sqrt{2/21}$	$-\mathrm{i}T_{\pi\sigma}\sqrt{2/42}$	0
$^3[\mathrm{f}_{-3}\,\mathrm{d}_{z^2}]S_1(-1)$	0	0	0	0
$^1[\mathrm{f}_3\,\mathrm{d}_{z^2}]S_0$	$T_{\pi\sigma}\sqrt{6/21}$	0	0	$-\mathrm{i}T_{\pi\sigma}\sqrt{6/42}$
$^1[\mathrm{f}_2\,\mathrm{d}_{z^2}]S_0$	$-\mathrm{i}T_{\pi\sigma}/42$	$-\mathrm{i}T_{\pi\sigma}5/42$	$T_{\pi\sigma}5/21$	$T_{\pi\sigma}/21$
$^1[\mathrm{f}_1\,\mathrm{d}_{z^2}]S_0$	0	$T_{\pi\sigma}\sqrt{10/21}$	$-\mathrm{i}T_{\pi\sigma}\sqrt{10/42}$	0
$^1[\mathrm{f}_0\,\mathrm{d}_{z^2}]S_0$	0	0	0	0
$^1[\mathrm{f}_{-1}\,\mathrm{d}_{z^2}]S_0$	$-T_{\pi\sigma}\sqrt{10/21}$	0	0	$\mathrm{i}T_{\pi\sigma}\sqrt{10/42}$
$^1[\mathrm{f}_{-2}\,\mathrm{d}_{z^2}]S_0$	$\mathrm{i}T_{\pi\sigma}5/42$	$\mathrm{i}T_{\pi\sigma}/42$	$-T_{\pi\sigma}/21$	$-T_{\pi\sigma}5/21$
$^1[\mathrm{f}_{-3}\,\mathrm{d}_{z^2}]S_0$	0	$-T_{\pi\sigma}\sqrt{6/21}$	$\mathrm{i}T_{\pi\sigma}\sqrt{6/42}$	0
$^3[\mathrm{f}_3\,\mathrm{d}_{x^2-y^2}]S_1(1)$	0	0	0	0
$^3[\mathrm{f}_2\,\mathrm{d}_{x^2-y^2}]S_1(1)$	0	0	0	$-\mathrm{i}T_{\pi\sigma}\sqrt{6/42}$
$^3[\mathrm{f}_1\,\mathrm{d}_{x^2-y^2}]S_1(1)$	0	$-\mathrm{i}T_{\pi\sigma}\sqrt{15/21}$	0	0
$^3[\mathrm{f}_0\,\mathrm{d}_{x^2-y^2}]S_1(1)$	0	0	0	0
$^3[\mathrm{f}_{-1}\,\mathrm{d}_{x^2-y^2}]S_1(1)$	0	0	0	0

Table 6. (Continued)

$Q_{mn}(\mathrm{A} \to \mathrm{B})$ charge transfer states	Ground state			
	$\varphi_A^+\varphi_B^+$	$\varphi_A^-\varphi_B^-$	$\varphi_A^+\varphi_B^-$	$\varphi_A^-\varphi_B^+$
$^3[\mathrm{f}_{-2}\,\mathrm{d}_{x^2-y^2}]S_1(1)$	0	0	0	$\mathrm{i}T_{\pi\sigma}\sqrt{150}/42$
$^3[\mathrm{f}_{-3}\,\mathrm{d}_{x^2-y^2}]S_1(1)$	0	$\mathrm{i}T_{\pi\sigma}/7$	0	0
$^3[\mathrm{f}_{3}\,\mathrm{d}_{x^2-y^2}]S_1(0)$	0	0	0	$\mathrm{i}T_{\pi\sigma}\sqrt{2}/14$
$^3[\mathrm{f}_{2}\,\mathrm{d}_{x^2-y^2}]S_1(0)$	$-\mathrm{i}T_{\pi\sigma}\sqrt{3}/42$	$\mathrm{i}T_{\pi\sigma}\sqrt{75}/42$	0	0
$^3[\mathrm{f}_{1}\,\mathrm{d}_{x^2-y^2}]S_1(0)$	0	0	$-\mathrm{i}T_{\pi\sigma}\sqrt{30}/42$	0
$^3[\mathrm{f}_{0}\,\mathrm{d}_{x^2-y^2}]S_1(0)$	0	0	0	0
$^3[\mathrm{f}_{-1}\,\mathrm{d}_{x^2-y^2}]S_1(0)$	0	0	0	$-\mathrm{i}T_{\pi\sigma}\sqrt{30}/42$
$^3[\mathrm{f}_{-2}\,\mathrm{d}_{x^2-y^2}]S_1(0)$	$\mathrm{i}T_{\pi\sigma}\sqrt{75}/42$	$-\mathrm{i}T_{\pi\sigma}\sqrt{3}/42$	0	0
$^3[\mathrm{f}_{-3}\,\mathrm{d}_{x^2-y^2}]S_1(0)$	0	0	$\mathrm{i}T_{\pi\sigma}\sqrt{2}/14$	0
$^3[\mathrm{f}_{3}\,\mathrm{d}_{x^2-y^2}]S_1(-1)$	$T_{\pi\sigma}/7$	0	0	0
$^3[\mathrm{f}_{2}\,\mathrm{d}_{x^2-y^2}]S_1(-1)$	0	0	$\mathrm{i}T_{\pi\sigma}\sqrt{150}/42$	0
$^3[\mathrm{f}_{1}\,\mathrm{d}_{x^2-y^2}]S_1(-1)$	0	0	0	0
$^3[\mathrm{f}_{0}\,\mathrm{d}_{x^2-y^2}]S_1(-1)$	0	0	0	0
$^3[\mathrm{f}_{-1}\,\mathrm{d}_{x^2-y^2}]S_1(-1)$	$-\mathrm{i}T_{\pi\sigma}\sqrt{15}/21$	0	0	0
$^3[\mathrm{f}_{-2}\,\mathrm{d}_{x^2-y^2}]S_1(-1)$	0	0	$-\mathrm{i}T_{\pi\sigma}\sqrt{6}/42$	0
$^3[\mathrm{f}_{-3}\,\mathrm{d}_{x^2-y^2}]S_1(-1)$	0	0	0	0
$^1[\mathrm{f}_{3}\,\mathrm{d}_{x^2-y^2}]S_0$	0	0	0	$-\mathrm{i}T_{\pi\sigma}\sqrt{2}/14$
$^1[\mathrm{f}_{2}\,\mathrm{d}_{x^2-y^2}]S_0$	$-\mathrm{i}T_{\pi\sigma}\sqrt{3}/42$	$-\mathrm{i}T_{\pi\sigma}\sqrt{75}/42$	0	0
$^1[\mathrm{f}_{1}\,\mathrm{d}_{x^2-y^2}]S_0$	0	0	$-\mathrm{i}T_{\pi\sigma}\sqrt{30}/42$	0
$^1[\mathrm{f}_{0}\,\mathrm{d}_{x^2-y^2}]S_0$	0	0	0	0
$^1[\mathrm{f}_{-1}\,\mathrm{d}_{x^2-y^2}]S_0$	0	0	0	$\mathrm{i}T_{\pi\sigma}\sqrt{30}/42$
$^1[\mathrm{f}_{-2}\,\mathrm{d}_{x^2-y^2}]S_0$	$\mathrm{i}T_{\pi\sigma}\sqrt{75}/42$	$\mathrm{i}T_{\pi\sigma}\sqrt{3}/42$	0	0
$^1[\mathrm{f}_{-3}\,\mathrm{d}_{x^2-y^2}]S_0$	0	0	$\mathrm{i}T_{\pi\sigma}\sqrt{2}/14$	0

All $\langle\varphi_A^{\pm}\varphi_B^{\pm}|\mathbf{H}_{AB}|Q_{mn}(\mathrm{A}\to\mathrm{B})\rangle$ matrix elements involving the d_{yz} orbital vanish.

$$a = \frac{J_{\pi\sigma}}{2} - \frac{J_{\pi\pi}}{2} \qquad b = \frac{J_{\pi\sigma}}{2} \qquad c = d = -\mathrm{i}\frac{J_{\pi\sigma}}{4} \tag{34}$$

where

$$J_{\pi\sigma} = \frac{40T_{\pi\sigma}^2}{441}\left(\frac{1}{U_{fd} - I_{fd} + 6Dq} - \frac{1}{U_{fd} + 6Dq}\right) \approx \frac{40}{441}\frac{T_{\pi\sigma}^2 I_{fd}}{(U_{fd} + 6Dq)^2} \tag{35a}$$

$$J_{\pi\pi} = \frac{80T_{\pi\pi}^2}{441}\left(\frac{1}{U_{fd} - I_{fd} - 4Dq} - \frac{1}{U_{fd} - 4Dq}\right) \approx \frac{80}{441}\frac{T_{\pi\pi}^2 I_{fd}}{(U_{fd} - 4Dq)^2}. \tag{35b}$$

Using equation (17) we find the exchange parameters of the spin-Hamiltonian (16) of the M_2L_{10} dimer

$$\begin{aligned} &J_x = J_{\pi\sigma} - \frac{J_{\pi\pi}}{2} \qquad J_y = \frac{J_{\pi\pi}}{2} \qquad J_z = \frac{J_{\pi\pi}}{2} \\ &D_{yz} = \frac{J_{\pi\sigma}}{2} \qquad D_{xy} = D_{xz} = 0 \qquad A_x = A_y = A_z = 0. \end{aligned} \tag{36}$$

It is seen from (36) that the resulting spin Hamiltonian of the M_2L_{10} f^1–f^1 dimer contains the non-diagonal terms $D_{\mu\nu}S_A^{\mu}S_B^{\nu}$. To diagonalize this spin Hamiltonian, we transform the

x, y and z axes to new x', y' and z' axes by an anticlockwise rotation about the x axis by the angle 45° as shown in figure 6. Upon this rotation S_n^μ components transform as

$$S_n^y = \frac{1}{\sqrt{2}}(S_n^{y'} + S_n^{z'}) \qquad S_n^x = S_n^{x'} \qquad S_n^z = \frac{1}{\sqrt{2}}(S_n^{y'} - S_n^{z'}). \tag{37}$$

Omitting the spin-independent term $(X+Y)/2$, we finally have

$$\mathbf{H} = J'_{x'} S_A^{x'} S_B^{x'} + J'_{y'} S_A^{y'} S_B^{y'} + J'_{z'} S_A^{z'} S_B^{z'} \tag{38}$$

where

$$J'_{x'} = 2J_{\pi\sigma} - J_{\pi\pi} \qquad J'_{y'} = J_{\pi\sigma} + J_{\pi\pi} \qquad J'_{z'} = -J_{\pi\sigma} + J_{\pi\pi}. \tag{39}$$

The principal spin quantization axes x', y' and z' of the diagonalized spin Hamiltonian (38) are shown in figure 6.

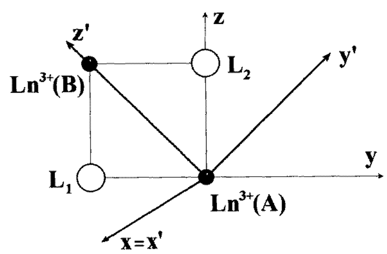

Figure 6. Spin quantization axes x', y' and z' of the diagonalized spin Hamiltonian of the M_2L_{10} f^1–f^1 dimer.

It can be seen from (38) and (39) that the anisotropy of the 90° f^1–f^1 superexchange is so pronounced that it is difficult to define whether the spin Hamiltonian (38) is antiferromagnetic or ferromagnetic because the exchange constants J_μ (39) may be of opposite sign,

$$\left.\begin{array}{l} J_{x'} > 0 \\ J_{y'} > 0 \\ J_{z'} < 0 \end{array}\right\} \text{ if } J_{\pi\sigma} > J_{\pi\pi} \qquad \left.\begin{array}{l} J_{x'} < 0 \\ J_{y'} > 0 \\ J_{z'} > 0 \end{array}\right\} \text{ if } J_{\pi\pi} > 2J_{\pi\sigma}. \tag{40}$$

It should be stressed that the contribution of an individual $Q_{mn}(\mathrm{A} \leftrightarrow \mathrm{B})$ charge-transfer state to the exchange parameters J_μ is of order $T_{\pi\sigma}^2/U_{fd}$, whereas the resulting exchange parameters (35) are of a smaller order of magnitude, $T_{\pi\sigma}^2 I_{fd}/U_{fd}^2$. It can be seen from (35) that the J_μ values are the sum of two terms of order $T_{\pi\sigma}^2/U_{fd}$ which are similar in magnitude but opposite in sign. This implies that all $Q_{mn}(\mathrm{A} \leftrightarrow \mathrm{B})$ states should be involved in the spin Hamiltonian calculation in order to obtain a physically consistent result.

3.4.2. The spin Hamiltonian for the M_2L_{11} dimer. The spin Hamiltonian of the M_2L_{11} f^1–f^1 dimer is derived by the same procedure as that employed above for the M_2L_{10} dimer. Again, using table 2 and transfer integrals from table 5, we calculate matrix elements $\langle \varphi_A^\pm \varphi_B^\pm | \mathbf{H}_{AB} | Q_{mn}(\mathrm{A} \leftrightarrow \mathrm{B})\rangle$ (table 7). Making use of equation (14), we have

$$X = -\frac{8T_{\pi\pi}^2}{441}\left(\frac{29}{U_{fd} - I_{fd} - 4Dq} + \frac{13}{U_{fd} - 4Dq}\right)$$
$$Y = -\frac{8T_{\pi\pi}^2}{441}\left(\frac{34}{U_{fd} - I_{fd} - 4Dq} + \frac{8}{U_{fd} - 4Dq}\right) \tag{41}$$

and $a = b = c = d = 0$.

Using (17) we find

$$J_x = J_y = 0 \qquad D_{xy} = D_{yz} = D_{xz} = 0 \qquad \mathbf{A} = 0 \qquad J_z = J_{\pi\pi} \tag{42}$$

where $J_{\pi\pi}$ is defined by (35*a*). Thus, we find that the 180° f^1–f^1 superexchange is anisotropic and described by the antiferromagnetic Ising spin Hamiltonian

$$\mathbf{H} = \frac{X + Y}{2} + J_{\pi\pi} S_A^z S_B^z \tag{43}$$

where the z axis direction connects ions A and B (figure 1(b)).

It can be seen from (35) that the CF splitting of 5d states $10Dq$ has a little influence on the exchange parameters, since $U_{fd} \gg Dq$. This is not surprising, because the CF potential does not couple 4f and 5d states due to its one-body nature.

3.5. Estimation of the f^1–f^1 superexchange parameters.

It is important to estimate the exchange parameters and to compare contributions of 4f5d and $4f^2$ configurations. We calculated $\langle 4f|2p\rangle$ and $\langle 5d|2p\rangle$ overlap integrals for oxide lanthanide compounds using radial wavefunctions for 4f lanthanide orbitals and 2p oxygen orbitals available in the literature [27, 28] and 5d lanthanide wavefunctions obtained from atomic X_α SW calculations. We found that the maximum overlaps are $S_\sigma(4f, 2p) \approx S_\pi(4f, 2p) = 0.02$–$0.03$, $S_\sigma(5d, 2p) = 0.15$ and $S_\pi(5d, 2p) = 0.1$, respectively. Employing the typical orbital energies $E(4f) = -7$ eV, $E(5d) = -5$ eV and $E(2p) = -15$ eV, we find from (33) that $T_{\pi\sigma} \approx T_{\pi\pi} = t(4f, 5d) \approx 0.1$ eV and $t(4f, 4f) \approx 0.02$–0.03 eV. Assuming that $U_{fd} = 10$ eV and $I_{fd} \approx G^1(4f, 5d) = 1$–$2$ eV we get an estimation

$$J \approx \frac{t(4f, 5d)^2 I_{fd}}{U_{fd}^2} = (1\text{–}2) \times 10^{-4}\ \text{eV} \approx 1\text{–}2\ \text{cm}^{-1} \tag{44}$$

which is quite consistent with the experimental exchange parameters normally observed in insulating lanthanide compounds [1–5]. Insofar as the role of 4f–4f charge transfers in the superexchange mechanism is concerned, the resulting exchange parameters of order $J \approx t^2(4f\text{–}4f)/U_{ff}$ are expected, where U_{ff} is the energy of the Coulomb repulsion between two 4f electrons on one lanthanide ion. This energy is estimated by $F^0(4f, 4f) \approx 10$ eV, so using $t(4f, 4f) = 0.02$–0.03 we have

$$J \approx \frac{t^2(4f, 4f)}{U_{ff}} = (4\text{–}9) \times 10^{-5}\ \text{eV} \approx 0.5\text{–}1\ \text{cm}^{-1}. \tag{45}$$

We can therefore conclude that the 4f–5d and 4f–4f charge-transfer processes give comparable contributions to the exchange parameters, so both these superexchange mechanisms should be taken into account. In this paper, however, only the 4f–5d mechanism has been considered.

In actinide compounds, 5f and 6d orbitals overlap with the ligand environment much better than lanthanide 4f and 5d orbitals do (this is especially true for tetravalent and pentavalent actinide compounds). As a consequence, similar calculations result in an estimation $J \approx 10$–30 cm^{-1}, which is consistent with the available experimental data (see below).

Table 7. $\langle\varphi_A^{\pm}\varphi_B^{\pm}|\mathbf{H}_{AB}|Q_{mn}(\mathrm{A}\to\mathrm{B})\rangle$ two-ion matrix elements for the M_2L_{11} dimer.

$Q_{mn}(\mathrm{A}\to\mathrm{B})$ charge transfer states	Ground state			
	$\varphi_A^+\varphi_B^+$	$\varphi_A^-\varphi_B^-$	$\varphi_A^+\varphi_B^-$	$\varphi_A^-\varphi_B^+$
$^3[f_3\ d_{zx}]S_1(1)$	0	0	0	0
$^3[f_2\ d_{zx}]S_1(1)$	0	0	0	$T_{\pi\pi}\sqrt{2/21}$
$^3[f_1\ d_{zx}]S_1(1)$	0	$T_{\pi\pi}\sqrt{20/21}$	0	0
$^3[f_0\ d_{zx}]S_1(1)$	0	0	0	0
$^3[f_{-1}\ d_{zx}]S_1(1)$	0	0	0	0
$^3[f_{-2}\ d_{zx}]S_1(1)$	0	0	0	$-T_{\pi\pi}\sqrt{50/21}$
$^3[f_{-3}\ d_{zx}]S_1(1)$	0	$-T_{\pi\pi}\sqrt{12/21}$	0	0
$^3[f_3\ d_{zx}]S_1(0)$	0	0	0	$-T_{\pi\pi}\sqrt{6/21}$
$^3[f_2\ d_{zx}]S_1(0)$	$-T_{\pi\pi}/21$	$-T_{\pi\pi}5/21$	0	0
$^3[f_1\ d_{zx}]S_1(0)$	0	0	$-T_{\pi\pi}\sqrt{10/21}$	0
$^3[f_0\ d_{zx}]S_1(0)$	0	0	0	0
$^3[f_{-1}\ d_{zx}]S_1(0)$	0	0	0	$T_{\pi\pi}\sqrt{10/21}$
$^3[f_{-2}\ d_{zx}]S_1(0)$	$T_{\pi\pi}5/21$	$T_{\pi\pi}/21$	0	0
$^3[f_{-3}\ d_{zx}]S_1(0)$	0	0	$T_{\pi\pi}\sqrt{6/21}$	0
$^3[f_3\ d_{zx}]S_1(-1)$	$T_{\pi\pi}\sqrt{12/21}$	0	0	0
$^3[f_2\ d_{zx}]S_1(-1)$	0	0	$T_{\pi\pi}\sqrt{50/21}$	0
$^3[f_1\ d_{zx}]S_1(-1)$	0	0	0	0
$^3[f_0\ d_{zx}]S_1(-1)$	0	0	0	0
$^3[f_{-1}\ d_{zx}]S_1(-1)$	$-T_{\pi\pi}\sqrt{20/21}$	0	0	0
$^3[f_{-2}\ d_{zx}]S_1(-1)$	0	0	$-T_{\pi\pi}\sqrt{2/21}$	0
$^3[f_{-3}\ d_{zx}]S_1(-1)$	0	0	0	0
$^1[f_3\ d_{zx}]S_0$	0	0	0	$T_{\pi\pi}\sqrt{6/21}$
$^1[f_2\ d_{zx}]S_0$	$-T_{\pi\pi}/21$	$T_{\pi\pi}5/21$	0	0
$^1[f_1\ d_{zx}]S_0$	0	0	$-T_{\pi\pi}\sqrt{10/21}$	0
$^1[f_0\ d_{zx}]S_0$	0	0	0	0
$^1[f_{-1}\ d_{zx}]S_0$	0	0	0	$-T_{\pi\pi}\sqrt{10/21}$
$^1[f_{-2}\ d_{zx}]S_0$	$T_{\pi\pi}5/21$	$-T_{\pi\pi}/21$	0	0
$^1[f_{-3}\ d_{zx}]S_0$	0	0	$T_{\pi\pi}\sqrt{6/21}$	0
$^3[f_3\ d_{yz}]S_1(1)$	0	0	0	0
$^3[f_2\ d_{yz}]S_1(1)$	0	0	0	$-\mathrm{i}T_{\pi\pi}\sqrt{2/21}$
$^3[f_1\ d_{yz}]S_1(1)$	0	$-\mathrm{i}T_{\pi\pi}\sqrt{20/21}$	0	0
$^3[f_0\ d_{yz}]S_1(1)$	0	0	0	0
$^3[f_{-1}\ d_{yz}]S_1(1)$	0	0	0	0
$^3[f_{-2}\ d_{yz}]S_1(1)$	0	0	0	$\mathrm{i}T_{\pi\pi}\sqrt{50/21}$
$^3[f_{-3}\ d_{yz}]S_1(1)$	0	$\mathrm{i}T_{\pi\pi}\sqrt{12/21}$	0	0
$^3[f_3\ d_{yz}]S_1(0)$	0	0	0	$\mathrm{i}T_{\pi\pi}\sqrt{6/21}$
$^3[f_2\ d_{yz}]S_1(0)$	$-\mathrm{i}T_{\pi\pi}/21$	$\mathrm{i}T_{\pi\pi}5/21$	0	0
$^3[f_1\ d_{yz}]S_1(0)$	0	0	$-\mathrm{i}T_{\pi\pi}\sqrt{10/21}$	0
$^3[f_0\ d_{yz}]S_1(0)$	0	0	0	0
$^3[f_{-1}\ d_{yz}]S_1(0)$	0	0	0	$-\mathrm{i}T_{\pi\pi}\sqrt{10/21}$
$^3[f_{-2}\ d_{yz}]S_1(0)$	$\mathrm{i}T_{\pi\pi}5/21$	$-\mathrm{i}T_{\pi\pi}/21$	0	0
$^3[f_{-3}\ d_{yz}]S_1(0)$	0	0	$\mathrm{i}T_{\pi\pi}\sqrt{6/21}$	0
$^3[f_3\ d_{yz}]S_1(-1)$	$\mathrm{i}T_{\pi\pi}\sqrt{12/21}$	0	0	0
$^3[f_2\ d_{yz}]S_1(-1)$	0	0	$\mathrm{i}T_{\pi\pi}\sqrt{50/21}$	0
$^3[f_1\ d_{yz}]S_1(-1)$	0	0	0	0
$^3[f_0\ d_{yz}]S_1(-1)$	0	0	0	0

Table 7. (Continued)

Q_{mn}(A → B) charge transfer states	Ground state			
	$\varphi_A^+\varphi_B^+$	$\varphi_A^-\varphi_B^-$	$\varphi_A^+\varphi_B^-$	$\varphi_A^-\varphi_B^+$
$^3[\mathrm{f}_{-1}\,\mathrm{d}_{yz}]S_1(-1)$	$-\mathrm{i}T_{\pi\pi}\sqrt{20/21}$	0	0	0
$^3[\mathrm{f}_{-2}\,\mathrm{d}_{yz}]S_1(-1)$	0	0	$-\mathrm{i}T_{\pi\pi}\sqrt{2/21}$	0
$^3[\mathrm{f}_{-3}\,\mathrm{d}_{yz}]S_1(-1)$	0	0	0	0
$^1[\mathrm{f}_3\,\mathrm{d}_{yz}]S_0$	0	0	0	$-\mathrm{i}T_{\pi\pi}\sqrt{6/21}$
$^1[\mathrm{f}_2\,\mathrm{d}_{yz}]S_0$	$-\mathrm{i}T_{\pi\pi}/21$	$-\mathrm{i}T_{\pi\pi}5/21$	0	0
$^1[\mathrm{f}_1\,\mathrm{d}_{yz}]S_0$	0	0	$-\mathrm{i}T_{\pi\pi}\sqrt{10/21}$	0
$^1[\mathrm{f}_0\,\mathrm{d}_{yz}]S_0$	0	0	0	0
$^1[\mathrm{f}_{-1}\,\mathrm{d}_{yz}]S_0$	0	0	0	$\mathrm{i}T_{\pi\pi}\sqrt{10/21}$
$^1[\mathrm{f}_{-2}\,\mathrm{d}_{yz}]S_0$	$\mathrm{i}T_{\pi\pi}5/21$	$\mathrm{i}T_{\pi\pi}/21$	0	0
$^1[\mathrm{f}_{-3}\,\mathrm{d}_{yz}]S_0$	0	0	$\mathrm{i}T_{\pi\pi}\sqrt{6/21}$	0

All $\langle\varphi_A^{\pm}\varphi_B^{\pm}|\mathbf{H}_{AB}|Q_{mn}(\mathrm{A}\to\mathrm{B})\rangle$ matrix elements involving the d_{z^2}, $\mathrm{d}_{x^2-y^2}$ or d_{xy} orbitals vanish.

4. Discussion

It can be seen from the above analysis that strong anisotropy of 90° and 180° f^1–f^1 superexchange is the result of a complex interplay of spin–orbit coupling, the CF effect, intra-ionic exchange and Coulomb interactions between 4f and 5d electrons, and anisotropic overlap between lanthanide 4f and 5d orbitals and np valent orbitals of the bridging ligands. It is seen from the comparison between the spin Hamiltonians (38) and (43) of the M_2L_{10} and M_2L_{11} dimers that the geometry of the dimer plays a decisive role in the f^1–f^1 superexchange mechanism. In particular, the Ln^{3+}–L–Ln^{3+} angles and good overlap between the lanthanide's and the ligand's orbitals in the dimers turns out to be even more important than the Ln^{3+}–Ln^{3+} distance. The symmetry of the ligand environment around the lanthanide ions is also important because the CF effect forms wavefunctions $\varphi_A^{\pm}$ and $\varphi_B^{\pm}$ of the ground Kramers doublets. These results show that a strong exchange anisotropy in f systems can occur even in the absence of the CF anisotropy and thus cannot be ascribed only to the latter. Further complications of the exchange mechanism are expected for low CF symmetries.

It should be noted once again that the spin Hamiltonian of the M_2L_{10} dimer is not additive with respect to two bridging ligands. This could be shown from two independent spin Hamiltonian calculations for the M_2L_{10} dimer with one of the bridging ligands removed. We found that the sum of two resulting spin Hamiltonians did not coincide with the total spin Hamiltonian (38).

It is interesting to discuss magnetic properties of some compounds containing f^1 ions in the light of the above results. Mixed uranium (V) oxides MUO_3 (where M = Li, Na, K or Rb) crystallize in the pervoskite-type structure, for which the M_2L_{11} dimer serves as a model cluster to describe the 180° superexchange interaction between two neighbouring $U^{5+}(5\mathrm{f}^1)$ ions. Similarly, the M_2L_{10} dimer is a model of the 90° f^1–f^1 superexchange in Li_3UO_4. This compound has a NaCl-type structure with a slight tetragonal distortion, in which cationic sites are occupied by Li^+ and U^{5+} ions in the ratio 3:1 [6, 7].

There is an interesting correlation between the structure and magnetic properties of the MUO_3 compounds. KUO_3 and $RbUO_3$ crystallize in a regular cubic perovskite structure and reveal no phase magnetic transitions in the magnetic susceptibility curves [7]. In contrast, $NaUO_3$ and $LiUO_3$ have distorted pervoskite structures [6, 7] and exhibit unusual magnetic properties. Thus, there is a magnetic phase transition at $T_N \approx 32$ K in $NaUO_3$ followed by a sharp peak in the magnetic susceptibility curve [6]. $LiUO_3$ has an unusual magnetic transition at $T_n \approx 19$ K which is accompanied by a rapid increase in the magnetic susceptibility in the vicinity of the transition point [29]. It is surprising that the magnetic susceptibilities of $NaUO_3$ and $LiUO_3$ below T_N depend on the applied magnetic field and increase with its increase [6, 7]. A very similar behaviour has recently been found in $BaPrO_3$ (orthorhombically distorted perovskite, $T_N = 11.5$ K) [30]. This magnetic behaviour is quite dissimilar to that of usual antiferromagnets and is indicative of strongly anisotropic $5f^1$–$5f^1$ exchange interactions in these compounds. Similar phenomena were also observed in Li_3UO_4 ($T_N \approx 6$ K) [29].

Unusual magnetic properties of these U (5+) and Pr (4+) oxides can be qualitatively rationalized in the light of the above results for the f^1–f^1 superexchange. The spin Hamiltonian of the high symmetry KUO_3 and $RbUO_3$ perovskites is obtained by a generalization of the 180° f^1–f^1 spin Hamiltonian (43),

$$\mathsf{H} = J_{\pi\pi} \sum_{\langle ij \rangle} \frac{(\boldsymbol{S}_i \cdot \boldsymbol{r}_{ij})(\boldsymbol{S}_j \cdot \boldsymbol{r}_{ij})}{|\boldsymbol{r}_{ij}|^2} \tag{46}$$

where the sum $\langle ij \rangle$ runs over all pairs of neighbouring f^1 ions in the simple cubic lattice and $\boldsymbol{r}_{ij} = \boldsymbol{r}_i - \boldsymbol{r}_j$ is a vector connecting ions i and j. The Hamiltonian (46) is formally antiferromagnetic and resembles the anisotropic part of the magnetic dipole–dipole Hamiltonian $\mu_A \mu_B / r_{AB}^3 - 3(\mu_A \boldsymbol{r}_{AB})(\mu_B \boldsymbol{r}_{AB})/r_{AB}^5$ albeit having the opposite sign and being of quite different origin. Although the ground state of this Hamiltonian is unknown, one has every reason to anticipate that spin fluctuations in this system are too strong for a magnetically ordered state to exist, as is the case in one- and two-dimensional antiferromagnets. We suggest therefore that this leads to the absence of magnetic ordering in KUO_3 and $RbUO_3$. In contrast, deviations from the regular perovskite structure in $LiUO_3$, $NaUO_3$ and $BaPrO_3$ would result in the appearance of the off-diagonal $D_{\mu\nu} S_i^\mu S_j^\nu$ and antisymmetrical $\mathbf{A}(\boldsymbol{S}_i \times \boldsymbol{S}_j)$ terms in the spin Hamiltonian which can cause magnetic ordering of a complex non-collinear spin structure. This suggestion gives a reasonable explanation of the field-dependence of the magnetic susceptibility in $LiUO_3$, $NaUO_3$ and $BaPrO_3$ below T_N, because an external magnetic field can have an effect on the angles between non-collinear magnetic moments of f^1 ions. A similar reason seems to be responsible for the magnetic properties of Li_3UO_4, whose exchange spin Hamiltonian is derived by a generalization of the spin Hamiltonian (43) and is therefore even more complicated than (46).

5. Conclusion

A modified superexchange theory has been developed and used for a quantitative study of exchange interactions between two f^1 ions bridged by common diamagnetic ligands. We have considered in detail the role of the CF effect, charge-transfer excited states A^+B^- and A^-B^+, and superexchange pathways for the simples M_2L_{10} and M_2L_{11} f^1–f^1 exchange dimers. Spin Hamiltonians of the 90° (M_2L_{10} dimer) and 180°(M_2L_{11}) f^1–f^1 superexchange are found to be extremely anisotropic. We have shown that this anisotropy is a result of a complex combination of spin–orbit coupling, the CF effect, intra-ionic electron–electron interactions and anisotropic overlaps between 4f and 5d lanthanide orbitals and np valent orbitals of the bridging ligands.

To understand more of the basics of exchange interaction in f systems, we tried to perform an analytical study for model systems rather than numerical calculations. However, further analysis of exchange interactions for many-electron f ions in actual lanthanide and actinide compounds demands the development of numerical techniques.

Acknowledgments

The author is indebted to Professor K W H Stevens for valuable discussions. This work was supported in part by the Russian Foundation for Fundamental Research, grant 95-02-06180a.

Appendix. Calculation of $\langle\varphi_A^{\pm}\varphi_B^{\pm}|\mathbf{H}_{AB}|Q_{mn}(A\rightarrow B)\rangle$ two-ion matrix elements

We illustrate the calculation procedure for the $\langle\varphi_A^{\pm}\varphi_B^{\pm}|\mathbf{H}_{AB}|Q_{mn}(\mathrm{A}\rightarrow \mathrm{B})\rangle$ two-ion matrix elements involved in (14). Consider a specific non-vanishing matrix element, say the $\langle\varphi_A^{+}\varphi_B^{+}|\mathbf{H}_{AB}|^3[\mathrm{f}_2\mathrm{d}_{z^2}]S_1(1)\rangle$ one for the M_2L_{10} dimer (table 6). Using table 2, we have

$$\begin{aligned}\langle\varphi_A^{+}\varphi_B^{+}|\mathbf{H}_{AB}|^3[\mathrm{f}_2\mathrm{d}_{z^2}]S_1(1)\rangle &= \langle(1/\sqrt{2})(\varphi_A^{+}(r_1,\sigma_1)\varphi_B^{+}(r_2,\sigma_2)\\ &\quad -\varphi_A^{+}(r_2,\sigma_2)\varphi_B^{+}(r_1,\sigma_1))|\mathbf{H}_{AB}|(1/\sqrt{2})(\mathrm{f}_2^B(\boldsymbol{r}_1)\,\mathrm{d}_{z^2}^B(\boldsymbol{r}_2)\\ &\quad -\mathrm{f}_2^B(\boldsymbol{r}_1)\,\mathrm{d}_{z^2}^B(\boldsymbol{r}_2))\alpha_1\alpha_2\rangle\\ &= \langle\varphi_A^{+}(\boldsymbol{r}_1,\sigma_1)\varphi_B^{+}(\boldsymbol{r}_2,\sigma_2)|\mathbf{H}_{AB}|\mathrm{f}_2^B(\boldsymbol{r}_1)\,\mathrm{d}_{z^2}^B(\boldsymbol{r}_2)\alpha_1\alpha_2\rangle\\ &\quad -\langle\varphi_A^{+}(\boldsymbol{r}_1,\sigma_1)\varphi_B^{+}(\boldsymbol{r}_2,\sigma_2)|\mathbf{H}_{AB}|\mathrm{f}_2^B(\boldsymbol{r}_2)\,\mathrm{d}_{z^2}^B(\boldsymbol{r}_1)\alpha_1\alpha_2\rangle \end{aligned} \tag{A.1}$$

Since $\mathbf{H}_{AB}$ is a one-electron operator, $\mathbf{H}_{AB} = \mathbf{h}_{AB}(1) + \mathbf{h}_{AB}(2)$, we can re-write (A.1) as

$$\begin{aligned}&\langle\varphi_A^{+}(\boldsymbol{r}_1,\sigma_1)|\mathbf{h}_{AB}(1)|\mathrm{f}_2^B(\boldsymbol{r}_1)\alpha_1\rangle\langle\varphi_B^{+}(\boldsymbol{r}_2,\sigma_2)|\,\mathrm{d}_{z^2}^B(\boldsymbol{r}_2)\alpha_2\rangle\\ &\quad +\langle\varphi_A^{+}(\boldsymbol{r}_1,\sigma_1)|\mathrm{f}_2^B(\boldsymbol{r}_1)\alpha_1\rangle\langle\varphi_B^{+}(\boldsymbol{r}_2,\sigma_2)|\mathbf{h}_{AB}(2)|\,\mathrm{d}_{z^2}^B(\boldsymbol{r}_2)\alpha_2\rangle\\ &\quad -\langle\varphi_A^{+}(\boldsymbol{r}_1,\sigma_1)|\mathbf{h}_{AB}(1)|\,\mathrm{d}_{z^2}^B(\boldsymbol{r}_1)\alpha_1\rangle\langle\varphi_B^{+}(\boldsymbol{r}_2,\sigma_2)|\mathrm{f}_2^B(\boldsymbol{r}_2)\alpha_2\rangle\\ &\quad -\langle\varphi_A^{+}(\boldsymbol{r}_1,\sigma_1)|\,\mathrm{d}_{z^2}^B(\boldsymbol{r}_1)\alpha_1\rangle\langle\varphi_B^{+}(\boldsymbol{r}_2,\sigma_2)|\mathbf{h}_{AB}(2)|\mathrm{f}_2^B(\boldsymbol{r}_2)\alpha_2\rangle. \end{aligned} \tag{A.2}$$

Because of the orthogonality relations $\langle\varphi_A^{+}(\boldsymbol{r}_1,\sigma_1)|\mathrm{f}_2^B(\boldsymbol{r}_1)\alpha_1\rangle = 0$ and $\langle\varphi_B^{+}(\boldsymbol{r}_2,\sigma_2)|\,\mathrm{d}_{z^2}^B(\boldsymbol{r}_2)\alpha_2\rangle = 0$, only the third term in (A.2) is retained:

$$\langle\varphi_A^{+}\varphi_B^{+}|\mathbf{H}_{AB}|^3[\mathrm{f}_2\,\mathrm{d}_{z^2}]S_1(1)\rangle = -\langle\varphi_A^{+}(\boldsymbol{r}_1,\sigma_1)|\mathbf{h}_{AB}(1)|\,\mathrm{d}_{z^2}^B(\boldsymbol{r}_1)\alpha_1\rangle\langle\varphi_B^{+}(\boldsymbol{r}_2,\sigma_2)|\mathrm{f}_2^B(\boldsymbol{r}_2)\alpha_2\rangle. \tag{A.3}$$

It is convenient to express $\varphi_A^{+}(\boldsymbol{r}_1,\sigma_1)$ via f orbitals of the cubic set and $\varphi_B^{+}(\boldsymbol{r}_2,\sigma_2)$ via the $|lm\rangle$ basis set from equation (28) in the text

$$\begin{aligned}\varphi_A^{+}(\boldsymbol{r}_1,\sigma_1) &= \frac{1}{\sqrt{21}}[2\mathrm{f}_{x(y^2-z^2)}^A(\boldsymbol{r}_1)\beta_1 + 2\mathrm{i}\mathrm{f}_{y(z^2-x^2)}^A(\boldsymbol{r}_1)\beta_1 - 3\mathrm{i}\mathrm{f}_{xyz}^A(\boldsymbol{r}_1)\alpha_1 + 2\mathrm{f}_{z(x^2-y^2)}^A(\boldsymbol{r}_1)\alpha_1]\\ \varphi_A^{+}(\boldsymbol{r}_2,\sigma_2) &= \frac{1}{\sqrt{42}}[\sqrt{6}\mathrm{f}_3^B(\boldsymbol{r}_2)\beta_2 - \mathrm{f}_2^B(\boldsymbol{r}_2)\alpha_2 - \sqrt{10}\mathrm{f}_{-1}^B(\boldsymbol{r}_2)\beta_2 + 5\mathrm{f}_{-2}^B(\boldsymbol{r}_2)\alpha_2]. \end{aligned} \tag{A.4}$$

Using the transfer integral $\langle\mathrm{f}_{z(x^2-y^2)}^A\alpha_1|\mathbf{h}_{AB}(1)|\,\mathrm{d}_{z^2}^B\alpha_1\rangle = T_{\pi\sigma}$ from table 4 we get

$$\langle\varphi_A^{+}(\boldsymbol{r}_1,\sigma_1)|\mathbf{h}_{AB}(1)|\,\mathrm{d}_{z^2}^B(\boldsymbol{r}_1)\alpha_1\rangle = \frac{2}{\sqrt{21}}T_\pi \qquad \langle\varphi_A^{+}(\boldsymbol{r}_2,\sigma_2)|\mathrm{f}_2^B(\boldsymbol{r}_2)\alpha_2\rangle = -\frac{1}{\sqrt{42}} \tag{A.5}$$

and, finally, we obtain

$$\langle\varphi_A^{+}\varphi_B^{-}|\mathbf{H}_{AB}|^3[\mathrm{f}_2\,\mathrm{d}_{z^2}]S_1(1)\rangle = \frac{\sqrt{2}}{21}T_{\pi\sigma}.$$

References

[1] Holmes L M, Van Uitert L G, Hecker R R *et al* 1972 *Phys. Rev.* B **5** 138
[2] Landau D P and Keen B E 1979 *Phys. Rev.* B **19** 4805
[3] Hansen P E, Johansson T and Nevald R 1975 *Phys. Rev.* B **12** 5315
[4] Riley J D, Baker J M and Birgeneau R J 1970 *Proc. R. Soc.* A **320** 369
[5] Cocharane R W, Wu C Y and Wolf W P 1972 *Phys. Rev.* B **8** 4348
[6] Miyake C, Takeuchi H, Fuji K and Imoto S 1984 *Phys. Status Solidi* a **83** 567
[7] Miyake C, Takeuchi H, Ohya-Nishiguchi H and Imoto S 1982 *Phys. Status Solidi* a **74** 173
[8] Maeda A and Sugimoto H 1986 *J. Chem. Soc. Faraday Trans.* **2** 82
[9] Hufner S 1978 *Optical Spectra of Transparent Rare Earth Compounds* (New York: Academic)
[10] Anderson P W 1959 *Phys. Rev.* **115** 2
[11] Anderson P W 1963 *Solid State Phys.* **14** 99
[12] Stevens K W H 1972 *J. Phys. C: Solid State Phys.* **5** 1360
[13] Veltruski I 1975 *Czech. J. Phys.* B **25** 101
[14] Stevens K W H 1976 *Phys. Lett.* C **24** 1
[15] Eremin M V 1982 *Sov. Phys. – Solid State* **24** 239
[16] Eremin M V 1983 *Sov. Phys. – Solid State* **25** 1010
[17] Furrer A, Gudel H U, Kransz E R and Blank H 1990 *Phys. Rev. Lett.* **64** 68
[18] Aebersold M A, Gudel H U, Hanser A, Furrer A and Blank H 1993 *Phys. Rev.* B **48** 12 723
[19] Goodenough J B 1976 *Magnetism and the Chemical Bond* (New York: Interscience)
[20] Kanamory J 1959 *J. Phys. Chem. Solids* **10** 87
[21] Wolfsberg M and Helmholz L 1952 *J. Chem. Phys.* **20** 837
[22] Feldkemper S, Weber W, Schulenburg J and Richter J 1995 *Phys. Rev.* B **52** 313
[23] Lee K R, Leask M J M and Wolf W P 1962 *J. Phys. Chem. Solids* **23** 1381
[24] Thornton G, Rosch N and Edelstein N 1980 *Inorg. Chem.* **19** 1303
[25] Mironov V S and Rosov S P 1991 *Phys. Status Solidi* b **170** 199
[26] Wybourne B G 1965 *Spectroscopic Properties of Rare Earth* (New York: Wiley)
[27] Declaux J P 1973 *At. Data Nucl. Data Tables* **12** 311
[28] McLean A D and McLean R S 1981 *At. Data Nucl. Data Tables* **26** 197
[29] 1971 *Lanthanides and Actinides MTP International Review of Science* vol 7 (London: Butterworth)
[30] Hinatsy Y 1993 *J. Solid State Chem.* **102** 362